U.S. DEPARTMENT OF COMMERCE
NATIONAL OCEANIC AND ATMOSPHERIC ADMINISTRATION
NATIONAL WEATHER SERVICE
NATIONAL METEOROLOGICAL CENTER

OFFICE NOTE 361

A COLUMBIA RIVER ENTRANCE WAVE FORECASTING PROGRAM DEVELOPMENT AT THE OCEAN PRODUCTS CENTER

Yung Y. Chao, and Tina L. Bertucci

October 1989

U.S. DEPARTMENT OF COMMERCE
NATIONAL OCEANIC AND ATMOSPHERIC ADMINISTRATION
OCEAN PRODUCTS CENTER

TECHNICAL NOTE*

A COLUMBIA RIVER ENTRANCE WAVE FORECASTING PROGRAM

DEVELOPED AT THE OCEAN PRODUCTS CENTER

YUNG Y. CHAO

AND

TINA L. BERTUCCI

OCTOBER 1989

OPC CONTRIBUTIONS

No. 1.   Burroughs, L. D., 1986: Development of Forecast Guidance for
         Santa Ana Conditions. National Weather Digest, Vol. 12 No. 1,
         8pp.

No. 2.   Richardson, W. S., D. J. Schwab, Y. Y. Chao, and D. M.
         Wright, 1986: Lake Erie Wave Height Forecasts Generated by
         Empirical and Dynamical Methods -- Comparison and Verification.
         Technical Note, 23pp.

No. 3.   Auer, S. J., 1986: Determination of Errors in LFM Forecasts
         Surface Lows Over the Northwest Atlantic Ocean. Technical
         Note/NMC Office Note No. 313, 17pp.

No. 4.   Rao, D. B., S. D. Steenrod, and B. V. Sanchez, 1987: A Method
         of Calculating the Total Flow from A Given Sea Surface
         Topography. NASA Technical Memorandum 87799., 19pp.

No. 5.   Feit, D. M., 1986: Compendium of Marine Meteorological
         and Oceanographic Products of the Ocean Products Center. NOAA
         Technical Memorandum NWS NMC 68, 93pp.

No. 6.   Auer, S. J., 1986: A Comparison of the LFM, Spectral, and
         ECMWF Numerical Model Forecasts of Deepening Oceanic Cyclones
         During One Cool Season. Technical Note/NMC Office Note No. 312,

No. 7.   Burroughs, L. D., 1987: Development of Open Fog Forecasting
         Regions. Technical Note/NMC Office Note. No. 323., 36pp.

No. 8.   Yu, T. W., 1987: A Technique of Deducing Wind Direction from
         Satellite Measurements of Wind Speed. Monthly Weather Review,
         Vol. 115, No. 9, pp1929-1939.

No. 9.   Auer, S. J., 1987: Five-Year Climatological Survey of the Gulf
         Stream System and Its Associated Rings. Journal of Geophysical
         Research, Vol. 92, No. C11, pp11,709-11,726.

No. 10. Chao, Y. Y., 1987: Forecasting Wave Conditions Affected by
         Currents and Bottom Topography. Technical Note, 11pp.

No. 11. Esteva, D. C., 1987: The Editing and Averaging of Altimeter Wave
         and Wind Data. Technical Note, 4pp.

No. 12. Feit, D. M., 1987: Forecasting Superstructure Icing for Alaskan
         Waters. National Weather Digest, Vol. 12 No. 2, pp5-10.

No. 13. Rao, D. B., B. V. Sanchez, S. D. Steenrod, 1987: Tidal
         Estimation in the Atlantic and Indian Oceans. Marine Geodesy,
         pp309-350. NASA Technical Memorandum 87812.

No. 14. Gemmill, W.H., T.W. Yu, and D.M. Feit 1988: Performance of
         Techniques Used to Derive Ocean Surface Winds. Technical Note/NMC
         Office Note No. 330, 34pp.

Table of Contents

List of Figures

A COLUMBIA RIVER ENTRANCE WAVE FORECASTING PROGRAM

DEVELOPED AT THE OCEAN PRODUCTS CENTER [1]

Y. Y. Chao and T. L. Bertucci

ABSTRACT

This report describes the OPC spectral wave forecasting model for the Columbia River Bar, as well as the results of some numerical experiments, on both micro and main frame computers. The model, essentially, calculates the transformation of offshore wave spectra forecasted by the OPC global wave model due to the combined effects of bottom topography and tidal currents in the vicinity of the Columbia River entrance.

INTRODUCTION

A marked change in the characteristics of ocean surface waves occurs due to the presence of prevailing currents and major bottom topographic features. A well known region characterized by intense and dramatic interactions of waves, currents and shoals is the Columbia River entrance on the west coast of the United States. It is recognized as one of the most dangerous coastal inlets in the world, where numerous search and rescue missions are conducted yearly by the Coast Guard and tragic losses of life continue to occur.

The National Weather Service(NWS, part of the National Oceanic and Atmospheric Administration, NOAA) is responsible for forecasting sea state conditions at potentially dangerous sites along the United States coastal areas. Presently, an analytical model developed by Gonzalez (1984) is used by the Seattle regional forecast office to generate guidance for forecasting wave conditions of the Columbia River Bar. The model is a one- dimensional current-bathymetry refraction model which assumes that waves are monochromatic, bottom contours are straight and parallel, and tidal

---

[1]OPC Contribution No.33

currents are unidirectional without lateral shear. The offshore source wave condition is determined by incorporating the information available from the synoptic weather forecast over the Pacific as well as wind and wave measurements at NDBC buoys.

Forecasts of the offshore wave conditions, including directional wave spectra, have been routinely issued by the OPC's global spectral ocean wave model through the AFOS network. It is desirable to take advantage of this information to provide an objective estimation of the offshore wave condition which is the required input for predicting waves near the river entrance. It is also desirable to have a two-dimensional representation of the highly irregular bottom configuration in the vicinity of the river entrance so that a more realistic specification of wave refraction effects can be made.

In an effort to provide objective forecast guidance for various coastal regions, a numerical forecasting model that uses the deep water spectral forecasts has been developed for the Columbia River entrance as a starting point. The model accounts for the refraction effects on waves caused by two-dimensional depth field and a unidirectional tidal current field. It was implemented on the NMC NAS9000 main frame computer. Recently, a PC version of the program has been prepared so that the regional forecasters can run the program locally. This report describes the underlying principle of the model and the numerical prediction procedure used. Also presented is a comparison of results obtained from the PC version, the main frame version, and the present regional office forecasts.

WAVE REFRACTION SPECIFICATION

The theory of wave refraction by current and bathymetry employs the dynamic and kinematic conservation principles and the dispersion relation as described in Phillips (1977). A comprehensive introduction to the general theory of ray tracing aplicable to various kinds of wave motions in liquids and gases is given by Lighthill(1978). Mathematical treatments of various wave-current interaction problems are discussed by Peregrine(1976).

The change of wave height under the influence of bathymetry and currents can be specified by the equation for the conservation of wave action or wave energy involving the radiation stresses. The equation for the conservation of wave action is preferable because of its computational simplicity.

The general conservation principle of wave action for a wave train has been estab-

lished by Bretherton and Garrett(1969) and can be expressed as

$$\frac{\partial}{\partial t}\left(\frac{E}{\sigma}\right) + \nabla \cdot \left\{ (\mathbf{C_g} + \mathbf{U})\frac{E}{\sigma} \right\} = 0 \tag{1}$$

Where E is the local wave energy per unit area(proportional to the square of the wave amplitude) and σ is the intrinsic frequency of the waves in a frame of reference moving with the local mean flow velocity $U(\mathbf{x}, t)$. The action density is defined as E/σ. For gravity water waves, the intrinsic frequency obeys the following dispersion relation

$$\sigma(k, h) = (gk \tanh kh)^{1/2} \tag{2}$$

where g is the gravitational acceleration, $h(\mathbf{x}, t)$ is the local water depth, $k = |\mathbf{k}|$, $\mathbf{k}(\mathbf{x}, t)$ the wave-number vector, and $\mathbf{C_g}$ represents the group velocity which can be found from the dispersion relation

$$\mathbf{C_g} = \frac{\partial \sigma}{\partial k}\left(\frac{\mathbf{k}}{k}\right) = \frac{1}{2}\frac{\sigma}{k}\left\{1 + \frac{2kh}{\sinh 2kh}\right\}\left(\frac{\mathbf{k}}{k}\right) \tag{3}$$

The actual sea surface displacement can be characterized by a continuous spectrum in the wave-number space. The spectral energy per unit area of a group of waves whose wave-number lie in the element of area δA of the wave-number plane,specified by the vectors $\mathbf{k}, \mathbf{k} + \delta\mathbf{k}'$, and $\mathbf{k} + \delta\mathbf{k}''$ is

$$E(\mathbf{k}) = \rho g F(\mathbf{k})\,\delta A \tag{4}$$

in which

$$\delta A = |\delta\mathbf{k}' \times \delta\mathbf{k}''| \tag{5}$$

where $F(\mathbf{k})$ is the spectral density and ρ the water density. Thus,in the absence of external forces which generate and/or dissipate the wave energy, the conservation equation for the action spectral energy can be expressed as

$$\frac{\partial}{\partial t}\left\{\frac{F(\mathbf{k})}{\sigma}\delta A\right\} + \nabla \cdot \left\{(\mathbf{C_g} + \mathbf{U})\frac{F(\mathbf{k})}{\sigma}\delta A\right\} = 0 \tag{6}$$

3

For each wave component, the apparent frequency, ω, in a stationary frame of reference is related to the intrinsic frequency by Doppler relationship

$$\omega(\mathbf{k}, \lambda) = \sigma + \mathbf{k} \cdot \mathbf{U} \tag{7}$$

where $\lambda(\mathbf{x}, t)$ is a parameter representing local properties of the medium, i.e., h and $\mathbf{U}$.

The wave refraction caused by variations in water depth and current, that is, changes of wave-number due to the medium nonhomogeneity, is specified by the kinematic conservation equation

$$\frac{\partial \mathbf{k}}{\partial t} + \nabla \omega = 0 \tag{8}$$

together with the irrotational condition of the wave-number

$$\nabla \times \mathbf{k} = 0 \tag{9}$$

Specifically, if we expand the spatial derivative in equation 8 and using equation 9, we obtain

$$\frac{dk_i}{dt} = -\frac{\partial \omega}{\partial \lambda} \frac{\partial \lambda}{\partial x_i} = -\frac{\partial \sigma}{\partial h} \frac{\partial h}{\partial x_i} - k_j \frac{\partial u_j}{\partial x_i} \tag{10}$$

where

$$\frac{d}{dt} \equiv \frac{\partial}{\partial t} + \frac{\partial \omega}{\partial k_j} \frac{\partial}{\partial x_j} \tag{11}$$

Here, we have used tensor summation convention to make involved relations easier to follow and defined $\mathbf{k} = (k_1, k_2)$, $\mathbf{C_g} = (c_{g1}, c_{g2})$, $\mathbf{U} = (u_1, u_2)$, $\mathbf{x} = (x_1, x_2)$ in a cartesian reference system.

The left-hand side of equation 10 represents the rate of change of k_i with time along the path transversed at the energy propagation velocity $c_{g_j} + u_j$, i.e.,

$$\frac{dx_j}{dt} = \frac{\partial \omega}{\partial k_j} = c_{g_j} + u_j \tag{12}$$

4

The path of energy propagation is called the characteristic curve or ray. By using equations 7 and 12, we obtain the rate of change of the apparent frequency, ω, with time along the ray. Since

$$\frac{\partial \omega}{\partial t} + \frac{\partial \omega}{\partial k_j} \frac{\partial \omega}{\partial x_j} =$$
$$\frac{\partial \omega}{\partial \lambda} \frac{\partial \lambda}{\partial t} + \frac{\partial \omega}{\partial k_i} \frac{\partial k_i}{\partial t} + \frac{\partial \omega}{\partial k_i} \left\{ \frac{\partial \omega}{\partial \lambda} \frac{\partial \lambda}{\partial x_j} + \frac{\partial \omega}{\partial k_i} \frac{\partial k_i}{\partial x_j} \right\} \tag{13}$$

and since from equation 10,the addition of the second term and terms involving the curly blakets in the right-hand side of the equation results in zero, we have

$$\frac{d\omega}{dt} = \frac{\partial \omega}{\partial \lambda} \frac{\partial \lambda}{\partial t} = \frac{\partial \sigma}{\partial h} \frac{\partial h}{\partial t} + k_i \frac{\partial u_i}{\partial t} \tag{14}$$

Equation 14 indicates that if water depth and current velocity do not vary with time, ω remains constant along each ray, which is a useful constraint for calculating refracted wave spectra at a specific location.

Equations 10, 12 and 14 are characteristic forms of kinematic results. The path of a ray is determined by simultaneous solution of this set of equations.

For practical calculations of ray trajectories, we need to take one more step. Let θ represents the direction of local wavenumber vector measured counterclockwise from the x_1-axis (e.g., from the east) and let $(k_1, k_2) = (k \cos \theta, k \sin \theta)$, $(u_1, u_2) = (u, v)$ and $(x_1, x_2) = (x, y)$. Equation 10 results in

$$\frac{dk}{dt} = -k \left(A \cos \theta + B \sin \theta \right) \tag{15}$$

and

$$\frac{d\theta}{dt} = A \sin \theta - B \cos \theta \tag{16}$$

where

$$A = \frac{1}{k} \frac{\partial \sigma}{\partial h} \frac{\partial h}{\partial x} + \cos \theta \frac{\partial u}{\partial x} + \sin \theta \frac{\partial v}{\partial x} \tag{17}$$

and

$$B = \frac{1}{k} \frac{\partial \sigma}{\partial h} \frac{\partial h}{\partial y} + \cos \theta \frac{\partial u}{\partial y} + \sin \theta \frac{\partial v}{\partial y} \tag{18}$$

and where

$$\frac{\partial \sigma}{\partial h} = \frac{\sigma}{h} \frac{kh}{\sinh 2kh} \tag{19}$$

5
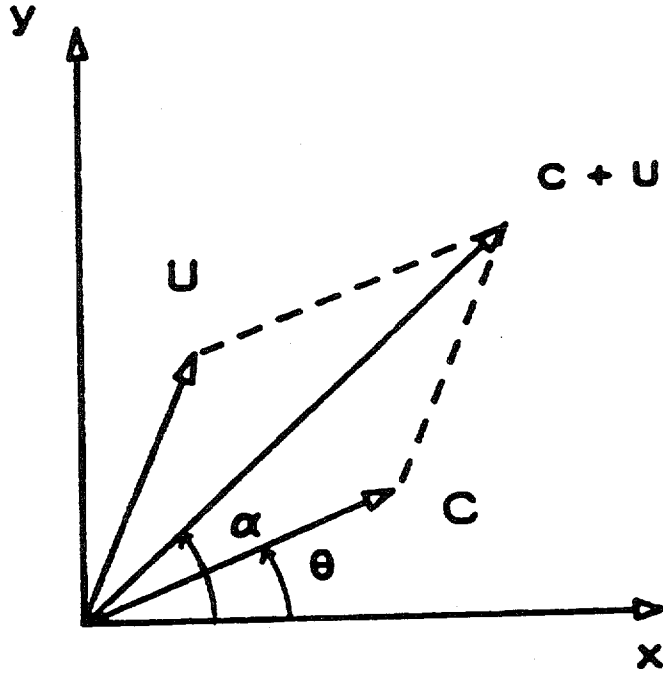
Figure 1: The vector orientation

It should be noted that, in the presence of current at a point along a ray, the direction of the local wave-number vector differs from the direction of wave energy propagation which is parallel to the ray direction. Let s be the arclength along a ray and $(c_{g_1}, c_{g_2}) = (c_g \cos\theta, c_g \sin\theta)$, where $c_g = |\mathbf{C_g}|$. Equation 12, then, can be expressed as

$$\frac{ds}{dt} = \{(c_g \cos\theta + u)^2 + (c_g \sin\theta + v)^2\}^{1/2} = |\mathbf{C_g} + \mathbf{U}| \qquad (20)$$

The ray direction (consequently the direction of energy propagation) is

$$\alpha = \tan^{-1}\left(\frac{c_g \sin\theta + v}{c_g \cos\theta + u}\right) \qquad (21)$$

The direction of wave-number vector is parallel to the ray only in the absence of current. A sketch of the directions of relevant vectors at a given time and point along a ray is shown in Figure 1. The commonly used term 'wave orthogonal' should not be confused with 'wave ray'. Orthogonals are lines in the direction of the wave-

number vector which is parpendicular to wave front while rays are paths traced out by 'wave action' points which move with the velocity $C_g + U$. These two terms coincide in the absence of currents.

Based on equation 8, Phillips(1977) has shown that the change of δA in equation 6 can be expressed as

$$\frac{\partial}{\partial t} \delta A + \nabla \cdot [(C_g + U) \delta A] = 0 \qquad (22)$$

From this equation and equation 6 we have

$$\left\{ \frac{\partial}{\partial t} + (C_g + U) \cdot \nabla \right\} \left(\frac{F(k)}{\sigma} \right) = 0 \qquad (23)$$

Equation 23 expresses that the action spectral density is conserved following a ray, i.e.

$$\frac{d}{dt} \left(\frac{F(k)}{\sigma} \right) = 0 \qquad (24)$$

In the absence of current, σ remains constant along the wave ray and so is the spectral density, $F(k)$. The result first demonstrated by Longuet-Higgins(1957).

In terms of variations in δA along a ray, equation 22 can be written as

$$\frac{d}{dt} \delta A = -\delta A \, \nabla \cdot (C_g + U) \qquad (25)$$

Equation 25 is not quite straightforward to solve. It cannot be directly integrated along a ray because knowledge of neighboring solutions is required to determine the divergence of the velocity on the right. To solve this problem, we follow the approach of Shen and Keller(1975) and introduce the Jacobian, $J(s,r)$ of the transformation from the ray coordinates (s,r) to $\mathbf{x} = (x,y)$,

$$J(s,r) = \frac{\partial(x,y)}{\partial(s,r)} \qquad (26)$$

7

where r is a parameter which is a constant on each ray(e.g., the initial infinitesimal distance between two neighboring rays) and s is the arclength along the ray given by equation 20. We then differentiate equation 26 with respect to s, to obtain [2]

$$\nabla \cdot (\mathbf{C_g} + \mathbf{U}) = |\mathbf{C_g} + \mathbf{U}| \left[\frac{1}{J}\frac{dJ}{ds} - |\mathbf{C_g} + \mathbf{U}|\frac{d}{ds}\left\{\frac{1}{|\mathbf{C_g} + \mathbf{U}|}\right\} \right] \tag{27}$$

Substituting this equation into equation 25 results in

$$\frac{d}{ds}\ln(J|\mathbf{C_g} + \mathbf{U}|\delta A) = 0 \tag{28}$$

i.e., $J|\mathbf{C_g} + \mathbf{U}|\,\delta A$ is conserved along a ray. The Jacobian $J(s,r)$ can be given a geometric interpretation. To do this, we note that the Jacobian defined by equation 26 can also be expressed as

$$J(s,r) = (0,0,1) \cdot \frac{\partial \mathbf{x}}{\partial s} \times \frac{\partial \mathbf{x}}{\partial r} \tag{29}$$

where $\partial \mathbf{x}/\partial s = \hat{s}$ is the unit tangent vector along a ray.

Thus

$$J(s,r)\,\delta r = \delta \nu \tag{30}$$

where

$$\delta \nu = \{\hat{s} \cdot \frac{\partial \mathbf{x}}{\partial r} \times (0,0,1)\}\delta r \tag{31}$$

is the width between two neighboring rays with parameter values r and $r+\delta r$. Since δr is a constant, we obtain from equations 24, and 28

$$\frac{F(\mathbf{k})}{\sigma}\{\delta \nu|\mathbf{C_g} + \mathbf{U}|\delta A\} = \frac{\mathbf{F'(k')}}{\sigma'}\{\delta \nu'|\mathbf{C_g}' + \mathbf{U}'|\delta A'\} \tag{32}$$

Here we have used prime (′) to designate parameters in the source area. Equation 32 shows that the wave action flux is conserved between two neighboring rays.

---

[2]See note at the end of this section.

The variance spectral component associated with the element of the wavenumber **k**, that contributes to the mean sea surface fluctuation at a specified location, is given by

$$F(\mathbf{k})\,\delta A = \frac{\sigma}{\sigma'} \left\{ \frac{\delta \nu'}{\delta \nu} \frac{|\mathbf{C_g}' + \mathbf{U}'|}{|\mathbf{C_g} + \mathbf{U}|} \right\} F'(\mathbf{k}')\,\delta A' = \frac{\sigma}{\sigma'} \left\{ \frac{\delta A}{\delta A'} \right\} F'(\mathbf{k}')\delta A' \qquad (33)$$

Munk and Arthur(1952) derived a second order differential equation to determine the change of the ray separation, $\delta \nu$, for wave refraction over a bottom of variable depth. Skvgaard and Jonsson(1976) extended the approach to include current effect. An alternate to determine the ray separation without recourse to solving the differential equation, however, can be made by evaluating the ratio $\delta A/\delta A'$ in the right-hand side of equation 33 in the following manner.

In this model, we assume that both the water depth and current velocity are slowly varing function of time in comparison with the variation in wave characteristics. Under this assumption, we may take advantage of the constancy of apparent wave frequency along the rays and consider the wave spectrum in the frequency- direction domain rather than the wavenumber space and replace $F(\mathbf{k})\delta A$ by $F(\omega, \theta)\delta\omega\delta\theta$. Since δA and $\delta\omega\delta\theta$ are related by the Jacobian as follows:

$$\frac{\delta A}{\delta \omega \delta \theta} = \frac{\partial(k_1, k_2)}{\partial(\omega, \theta)} = \frac{k}{c_g + u \cos \theta + v \sin \theta} \qquad (34)$$

Therefore,

$$\frac{\delta A}{\delta A'} = \frac{c_g' + u' \cos \theta' + v' \sin \theta'}{c_g + u \cos \theta + v \sin \theta} \frac{k}{k'} \frac{\delta \theta}{\delta \theta'} \qquad (35)$$

Consider a special case in which currents are absent, i.e., $\mathbf{U} = \mathbf{U}' = 0$, $\sigma = \sigma'$, and the bottom contours are straight and parallel to the shoreline such that $h = h(x)$. Since equation 20 reduces to $dt = ds/c_g = dx/(c_g \cos \theta)$, we combine equations 15 and 16 to obtain

$$\frac{d\theta}{dx} = -\frac{\tan \theta}{k} \frac{dk}{dx} \qquad (36)$$

From which we immediately have

9

$$\sin\theta / \sin\theta' = k'/k \qquad (37)$$

which is the well known Snell law. To the first order, we can write

$$\delta\theta = \frac{\partial\theta}{\partial\theta'}\delta\theta' \qquad (38)$$

Differentiating equation 37 with respect to θ and θ', we obtain

$$\frac{\delta\theta}{\delta\theta'} = \frac{k' \cos\theta'}{k \cos\theta} \qquad (39)$$

Thus,

$$\frac{\delta A}{\delta A'} = \frac{c_g'}{c_g} \frac{\cos\theta'}{\cos\theta} \equiv K_s^2 K_r^2 \qquad (40)$$

which is the clasical result for computing the wave height amplification of monocromatic waves obliquely incident on a beach with straight and parallel bottom contours. The term K_s is commonly called the shoaling coefficient and K_r the refraction coefficient(SPM, 1984). The relation $K_r^2 = (k/k')(\delta\theta/\delta\theta')$ has also been derived for bathymetric refraction of monocromatic waves by Dorrestein(1960) and by Le Méhauté and Wang(1982) for the wave spectrum.

Let $S(\omega_m, \theta_n, t_o)$ represents the variance spectrum at the forecast point over a band of frequencies and directions

$$S(\omega_m, \theta_n, t_o) = \int_{\omega_m - \Delta\omega/2}^{\omega_m + \Delta\omega/2} \left\{ \int_{\theta_n - \Delta\theta/2}^{\theta_n + \Delta\theta/2} F(\omega, \theta, t_o)d\theta \right\} d\omega \qquad (41)$$

In general, $S(\omega_m, \theta_n, t_o)$ will be given by a linear combination of some subset of the spectrum in the source region which will arrive at the forecast point at t_o so that

$$S(\omega_m, \theta_n, t_o) = \sum_i W_i F'(\omega_m, \theta'_{n+i}, t_o - \tau_i)\Delta\theta'_i \Delta\omega \qquad (42)$$

10

where τ is the time lag of a spectral element to propagte from the source to the forecast point, and where

$$W = \frac{\sigma}{\sigma'}\frac{\delta A}{\delta A'} = \frac{\sigma}{\sigma'}\left|\frac{c'_g + u'\cos\theta' + v'\sin\theta'}{c_g + u\cos\theta + v\sin\theta}\right|\frac{k}{k'}\left|\frac{\delta\theta}{\delta\theta'}\right| \qquad (43)$$

is the energy amplification factor.

Once the directional spectrum is determined, various wave parameters can be calculated. The mean square surface fluctuation $\overline{\eta^2}$ and the significant wave height $H_{1/3}$ at the forecast location are given by

$$\overline{\eta^2} = \sum_{m,n} S(\omega_m, \theta_n) \qquad (44)$$

and

$$H_{1/3} = 4\left(\overline{\eta^2}\right)^{1/2} \qquad (45)$$

respectively. The average zero up-crossing wave period, $\tilde{T}$, is determined from

$$\tilde{T} = 2\pi\left[\frac{\int F(\omega)\,d\omega}{\int \omega^2 F(\omega)\,d\omega}\right]^{1/2} \qquad (46)$$

where

$$F(\omega) = \int F(\omega, \theta)\,d\theta \qquad (47)$$

(For example, see Pierson and Neumann,1966).

It can be observed from equation 43 that the amplification factor may become unrealistically large when $|\delta\theta/\delta\theta'| \rightarrow \infty$ or when $(c_g + u\cos\theta + v\sin\theta) \rightarrow 0$. Treatments of these problems and the practical procedure for calculating the refracted spectrum are discussed in the succeeding sections.

11

Note Added in Proof of Equation 27

Since

$$
\begin{aligned}
\frac{dJ}{ds} &= \frac{d}{ds}\left\{\frac{\partial x}{\partial s}\frac{\partial y}{\partial r} - \frac{\partial x}{\partial r}\frac{\partial y}{\partial s}\right\} \\
&= \frac{\partial x}{\partial s}\frac{d}{ds}\left(\frac{\partial y}{\partial r}\right) + \frac{\partial y}{\partial r}\frac{d}{ds}\left(\frac{\partial x}{\partial s}\right) - \frac{\partial x}{\partial r}\frac{d}{ds}\left(\frac{\partial y}{\partial s}\right) - \frac{\partial y}{\partial s}\frac{d}{ds}\left(\frac{\partial x}{\partial r}\right) \\
&= \frac{\partial x}{\partial s}\frac{\partial}{\partial r}\left(\frac{dy}{ds}\right) + \frac{\partial y}{\partial r}\frac{\partial}{\partial s}\left(\frac{dx}{ds}\right) - \frac{\partial x}{\partial r}\frac{\partial}{\partial s}\left(\frac{dy}{ds}\right) - \frac{\partial y}{\partial s}\frac{\partial}{\partial r}\left(\frac{dx}{ds}\right) \\
&= \frac{\partial x}{\partial s}\left[\left\{\frac{\partial}{\partial y}\left(\frac{dy}{ds}\right)\right\}\frac{\partial y}{\partial r} + \left\{\frac{\partial}{\partial x}\left(\frac{dy}{ds}\right)\right\}\frac{\partial x}{\partial r}\right] + \\
&\quad \frac{\partial y}{\partial r}\left[\left\{\frac{\partial}{\partial y}\left(\frac{dx}{ds}\right)\right\}\frac{\partial y}{\partial s} + \left\{\frac{\partial}{\partial x}\left(\frac{dx}{ds}\right)\right\}\frac{\partial x}{\partial s}\right] - \\
&\quad \frac{\partial x}{\partial r}\left[\left\{\frac{\partial}{\partial y}\left(\frac{dy}{ds}\right)\right\}\frac{\partial y}{\partial s} + \left\{\frac{\partial}{\partial x}\left(\frac{dy}{ds}\right)\right\}\frac{\partial x}{\partial s}\right] - \\
&\quad \frac{\partial y}{\partial s}\left[\left\{\frac{\partial}{\partial y}\left(\frac{dx}{ds}\right)\right\}\frac{\partial y}{\partial r} + \left\{\frac{\partial}{\partial x}\left(\frac{dx}{ds}\right)\right\}\frac{\partial x}{\partial r}\right] \\
&= \left(\frac{\partial x}{\partial s}\frac{\partial y}{\partial r} - \frac{\partial x}{\partial r}\frac{\partial y}{\partial s}\right)\left\{\frac{\partial}{\partial x}\left(\frac{dx}{ds}\right) + \frac{\partial}{\partial y}\left(\frac{dy}{ds}\right)\right\} \\
&= J\left\{\frac{\partial}{\partial x}\left(\frac{dx}{dt}\frac{dt}{ds}\right) + \frac{\partial}{\partial y}\left(\frac{dy}{dt}\frac{dt}{ds}\right)\right\} \\
&= J\left[\frac{dt}{ds}\left\{\frac{\partial}{\partial x}\left(\frac{dx}{dt}\right) + \frac{\partial}{\partial y}\left(\frac{dy}{dt}\right)\right\} + \frac{dx}{dt}\frac{\partial}{\partial x}\left(\frac{dt}{ds}\right) + \frac{dy}{dt}\frac{\partial}{\partial y}\left(\frac{dt}{ds}\right)\right] \\
&= J\left[|\mathbf{C_g} + \mathbf{U}|^{-1}\nabla\cdot(\mathbf{C_g} + \mathbf{U}) + (\mathbf{C_g} + \mathbf{U})\cdot\nabla|\mathbf{C_g} + \mathbf{U}|^{-1}\right] \quad (48)
\end{aligned}
$$

and since for the steady state condition

$$
\frac{\partial}{\partial t}|\mathbf{C_g} + \mathbf{U}|^{-1} = 0 \quad (49)
$$

we have from equations 12 and 20

$$
(\mathbf{C_g} + \mathbf{U})\cdot\nabla|\mathbf{C_g} + \mathbf{U}|^{-1} = \frac{d}{dt}|\mathbf{C_g} + \mathbf{U}|^{-1} = |\mathbf{C_g} + \mathbf{U}|^{-1}\frac{d}{ds}|\mathbf{C_g} + \mathbf{U}|^{-1} \quad (50)
$$

Therefore, by substituting equation 50 to equation 48 and rearranging, we obtain

$$
\nabla\cdot(\mathbf{C_g} + \mathbf{U}) = |\mathbf{C_g} + \mathbf{U}|\left[\frac{1}{J}\frac{dJ}{ds} - |\mathbf{C_g} + \mathbf{U}|\frac{d}{ds}|\mathbf{C_g} + \mathbf{U}|^{-1}\right] \quad (51)
$$

THE REVERSE RAY TRACING

In determining the amplification factors for selected locations in water of varying depth , a traditional approach is to construct a number of rays from deep water so that as they travel toward the beach, there will have sufficient number of rays arrive at the area of interest. With complex topography, it is often very difficult to intuit which rays in deep water will ultimately pass close to the point of interest. Dorrestein (1960) has devised a method for tracing rays in the reverse direction from a point in the refraction zone backwards out into deep water. The method is especially convenient if one is interested in refraction effect at only one particular locality. The approach does not obtain a field of wave height everywhere in the entire water domain at a particular time. However, the rays so calculated are true for any choice of incident wave field, so the loss of spatial generality is compensated by an increase in temporal generality. This method is applied and extended in this model to include the current effects.

The computational procedure is as follows. For a given spectral frequency band, construct the ray path in the initial direction $\theta + 180°(mod\,360°)$ from the forecast point until the ray reaches offshore source wave region. At the source point, compute the ray travel time Δt , the angle θ' , and the coordinates, x' and y' . The wave number, the intrinsic frequency at both ends of the ray, also must be determined. These refraction parameters are calculated based on equations 2, 3, 7 and 15 through 19 given in the previous section. The wave-number along a ray can be computed from equation 14, but using an iterative scheme to determine the wavenumber from equation 7 is simpler. It should be noted that in performing reverse ray tracing with the presence of currents, the current direction must be reversed prior to calculation.

Rays are constructed in this manner for all spectral direction bands of interest (with additional directions in-between the neighboring bands, i.e., $\pm \triangle\theta/2$). The value of $|\delta\theta/\delta\theta'|$ corresponding to each direction band is then determined from the $\theta \sim \theta'$ curve. Figure 2 shows three possible type of $\theta \sim \theta'$ curves.

Usually, the wave direction at a forecast point would be a simple monotonic function of the source wave direction (Figure 2a). The situation corresponds to wave refraction on a linear sloping bottom of parallel contours or with the presence of linear shear currents. For this situation

$$\left|\frac{\delta\theta}{\delta\theta'}\right| \simeq \left|\frac{\theta_n - \theta_{n-1}}{\theta'(\theta_n) - \theta'(\theta_{n-1})}\right| \tag{52}$$

where $\theta_n - \theta_{n-1} = \triangle\theta/2$.

The discontinuous curve shown in Figure 2b corresponds to the situation where there is an island or a offshore breakwater which prevents waves arriving at the forecast point from a
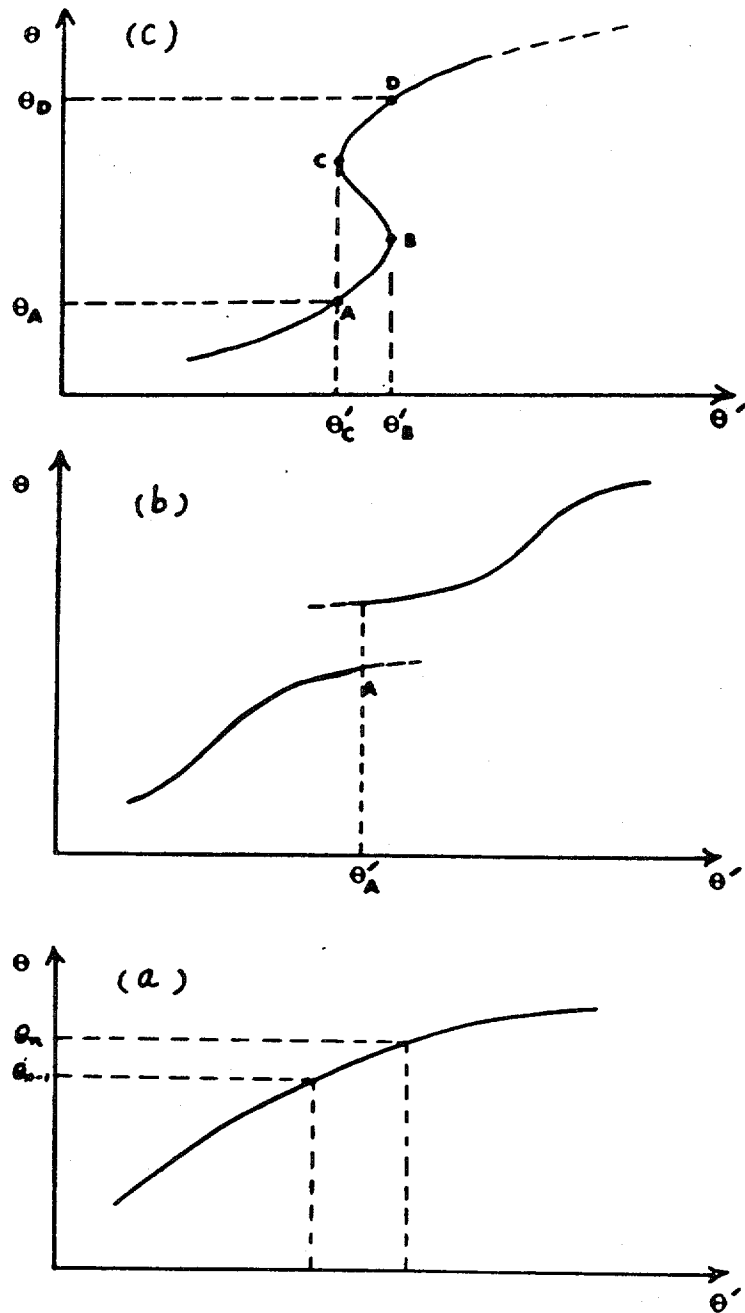
13

Figure 2: Three types of $\theta \sim \theta'$ curve.

certain range of directions or there exists a strong shear current which causes total reflection of waves back to source area. It may also corresponds to the case that waves from certain directions near θ'_A arriving at the forecast area from both sides of the island and forms a rhomboid wave patterns. The $|\delta\theta/\delta\theta'|$ value should be computed for each curve according to equation 52. For the interval of θ in which no value for θ' corresponds, the $|\delta\theta/\delta\theta'|$ value, of course, should be set to zero.

The smooth curve with multiple values of wave directions at the forecast point associated with a single incident wave direction at the source (Figure 2c) indicates that the point is lying in the caustic zone. A caustic is defined as the envelop of a set of wave rays emanates from a common source with identical characteristics. In the neighborhood of a caustic the ordinary ray method does not apply; a higher order theory involving Airy function is required (Chao, 1971). Dorrestein (1960) has proposed a crude yet simple procedure to treat this problem associated with the reverse ray tracing practice.

For a wave direction between θ_C' and θ_B' we have more than one corresponding wave direction at the forecast point. At points B and C, $|\delta\theta/\delta\theta'| = \infty$ and consequently, the amplification factor, $W = \infty$. Such a case occurs, for instance, if the rays pass a current field associated with a warm core ring (Mapp et al, 1985) or some shoal region which acts as a positive lens(Pierson, 1951). In figure 2c the points characterizing the rays which are then most influenced by this shoal region lie between B and C and a caustic zone is formed at the forecast point by waves coming from the directions θ_C' and θ_B'. For a spectral directional band lying within this angle range, the following approximation is proposed by Dorrestein(1960):

$$\left| \frac{\delta\theta}{\delta\theta'} \right| \simeq \left| \frac{\theta_D - \theta_A}{\theta_C'(\theta_A) - \theta_B'(\theta_D)} \right| \tag{53}$$

Computations by the same procedure are made once and for all frequency bands involved for the forecast point given the depth and current field around the point. The resulting refraction parameters which are needed for computing refracted spectra at the forecast point are saved as a permanent file. These parameters include θ', Δt, x' and y', and W. They are a function of ω, θ and $\mathbf{U}$ of the forecast point.

Calculations of the amplification factor for a simplified case were made to examine the consistency of the model and to compare the results with Gonzalez(1984) analytical solutions. the following was assumed: (1) water depth of 15 meters at the forecast point increased linearly to a depth of 60 meters ,(2) the flow direction was perpendicular to the bottom contours, and (3) the current speed varied linearly from a given value at the forecast point to zero at 60 meters depth.

Figure 3 shows examples of $\theta \sim \theta'$ curves, and $|\delta\theta/\delta\theta'|$ as well as the values of W as the function of θ, associated with various frequencies and current speeds. The negative sign on flow speed indicates that flow direction is from the forecast point toward offshore while the
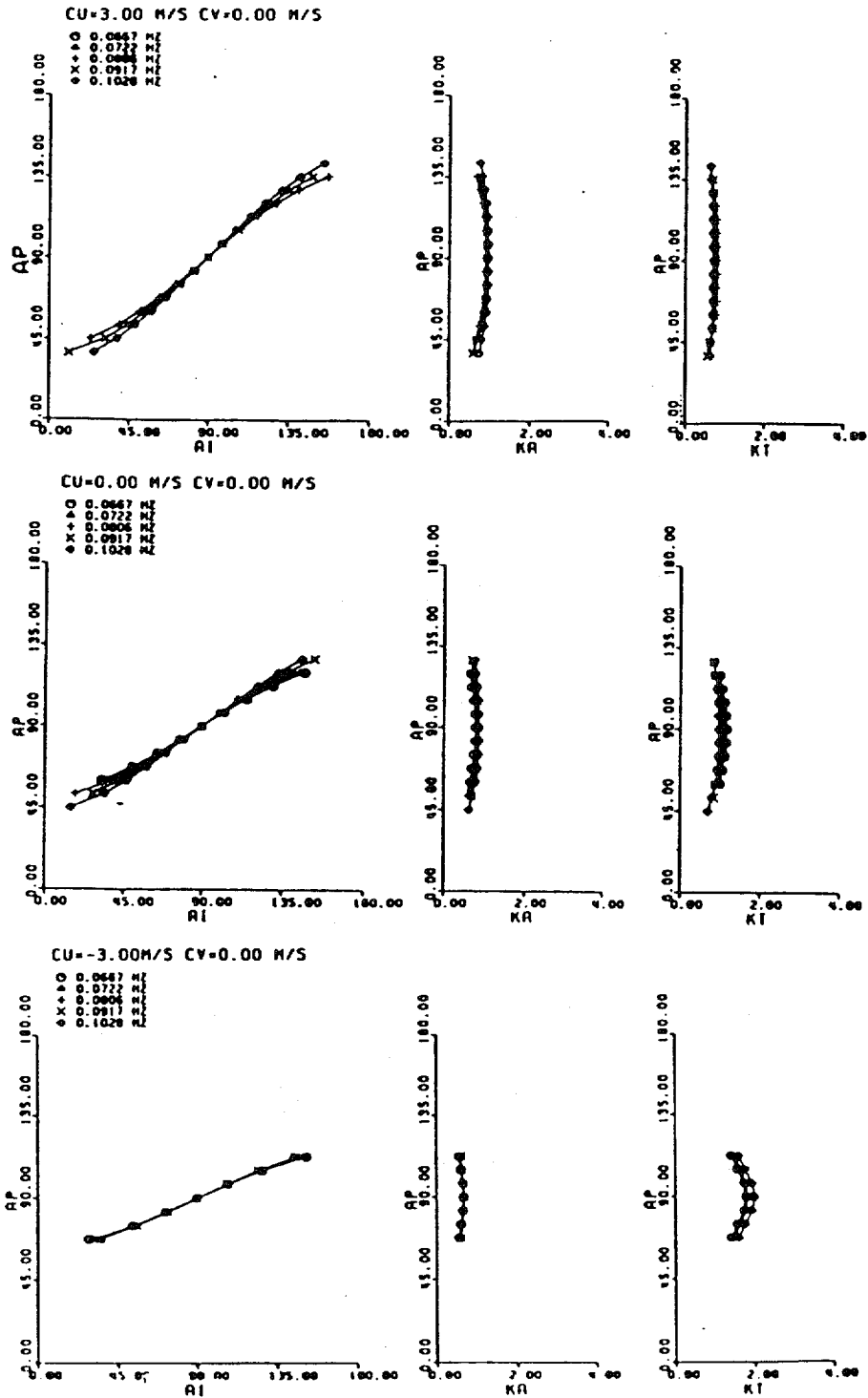
15

Figure 3: Examples of calculated refraction parameters for a linear sloping bottom associated with various frequencies and current speeds, where AP= θ=wave direction at the forecast point,AI=θ'=wave direction in the source region, KA=$|\delta\theta/\delta\theta'|$ and KT=W=the amplification factor.

positive sign indicates that the current are from offshore to the forecast point. All curves for $|\delta\theta/\delta\theta'|$ and for W in this figure are symmetric to $\theta = 90°$. This is as expected because the angle is in the direction perpendicular (parallel) to the bottom contours (the current direction).

Figure 4, 5 and 6 compares numerical and analytical results of the amplification factor for wave incidence angle of 0, 30 and 60 degrees with respect to the flow direction. For the case that the incidence angle is parallel to the flow direction , the numerical solution is almost identical with the analytical one. For the case of large incidence angle, the numerical result begins to deviate from the analytical solution, particularly with strong opposing currents. The numerical results presented are calculated based on an angular increment of 7.5 degrees. Accuracy may be improved if a smaller angular interval is used.

THE LIMITING WAVE SPECTRUM

The problem of $c_g + u\cos\theta + v\sin\theta = 0$ in Equation 42 implies that the local wave group velocity is equal and opposite to the flow velocity and energy can no longer be propagated against the stream. The simplest example is the incidence of a wave train moving in the x - direction on a variable current $U(x)$ in deep water. The current velocity required to satisfy the condition is only one-quater of the phase velocity of waves in still water, i.e.,$U = -g/(4\omega)$ (Phillips, 1977). For a wave of 5 sec period, the required velocity is theoretically 2 m/sec. It is commonly assumed that waves break shortly before reaching this point. Upstream of such points, especially if the current slackens, the water surface will be considerbly smooth as all short waves are eliminated. The cutoff frequency is $\omega = g/(4U)$. The components with frequencies greater than $g/(4U)$ are not transmitted at all. This velocity is called the "stopping velocity" and is corresponding to a caustic (the envelope of a set of rays). It is possible for the waves to be reflected and swept downstream, as shorter waves, by the current. Perrgrine(1976) has discussed solutions in the neighborhood of the caustic corresponds to the stopping velocity for the case of unidirectional flow in deep water. A simplified treatment of the caustic problem occured in the reverse ray tracing method has been described in a previous section and will not be concerned here.

In addition to possible breaks of waves propagating in an adverse current, wave breaking also occur as waves move into water sufficiently shallow. The problem to be considered, therefore, is what criterion has to impose on the increase of energy as waves encounter an adverse current in water of finite depth so that the predicted spectraum is realistic. There are various rule of thumb equations for the maximum wave height or wave spectrum in water of finite depth but equations which also involves current effects are rare. Recently, Tung and Huang(1987) devise a method to compute the spectrum of waves in water of finite depth taking into account the effect of wave breaking in the presence of current. The expressions derived is extremely complex and the result of calculation for simplified current

17

COMPARISON OF ANALYTICAL & NUMERICAL
SOLUTION FOR INCIDENT ANGLE = 0 DEGREE

U=-2.5 m/s

U=-1.5 m/s

U=0.0 m/s

U=+2.5 m/s

AMPLIFICATION FACTOR

FREQUENCY (Hz)

Figure 4: Comparison of numerical and anlytical solutions(solid lines) of the amplification
factors for 0 degree incident wave directions.

18

COMPARISON OF ANALYTICAL & NUMERICAL
SOLUTION FOR INCIDENT ANGLE = 30 DEGREES

Figure 5: Comparison of numerical and anlytical solutions(solid lines) of the amplification factors for 30 degree incident wave directions.

19

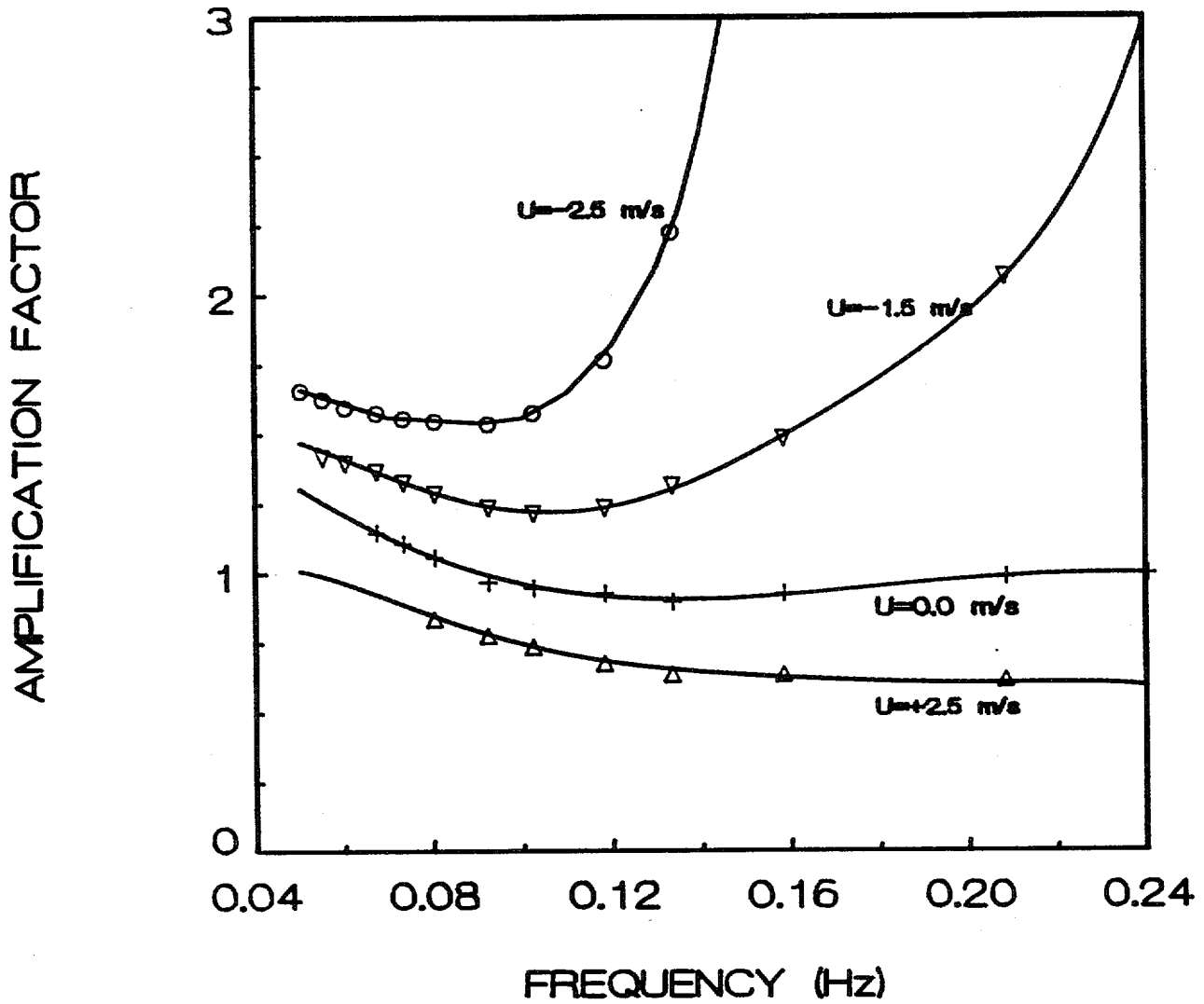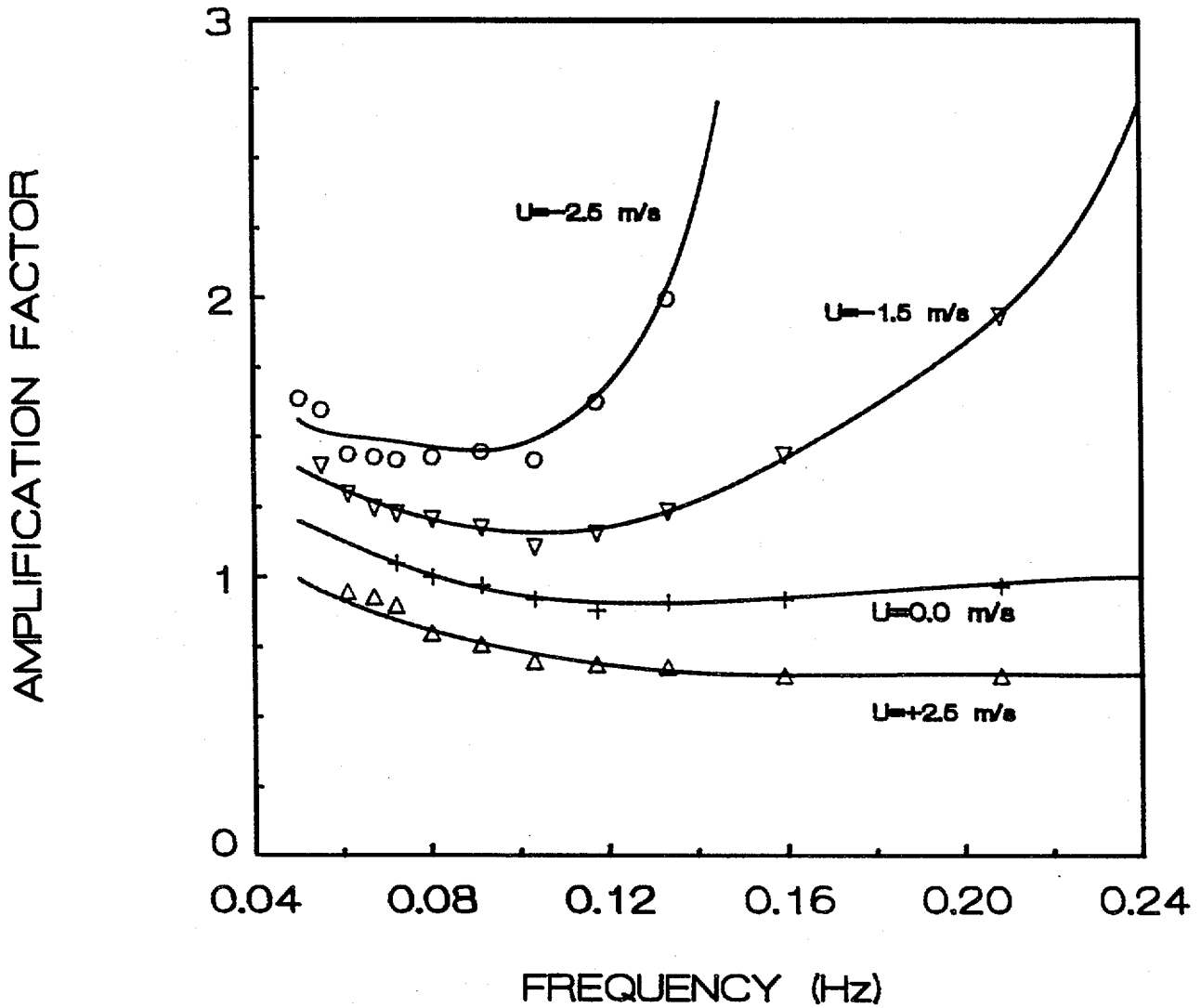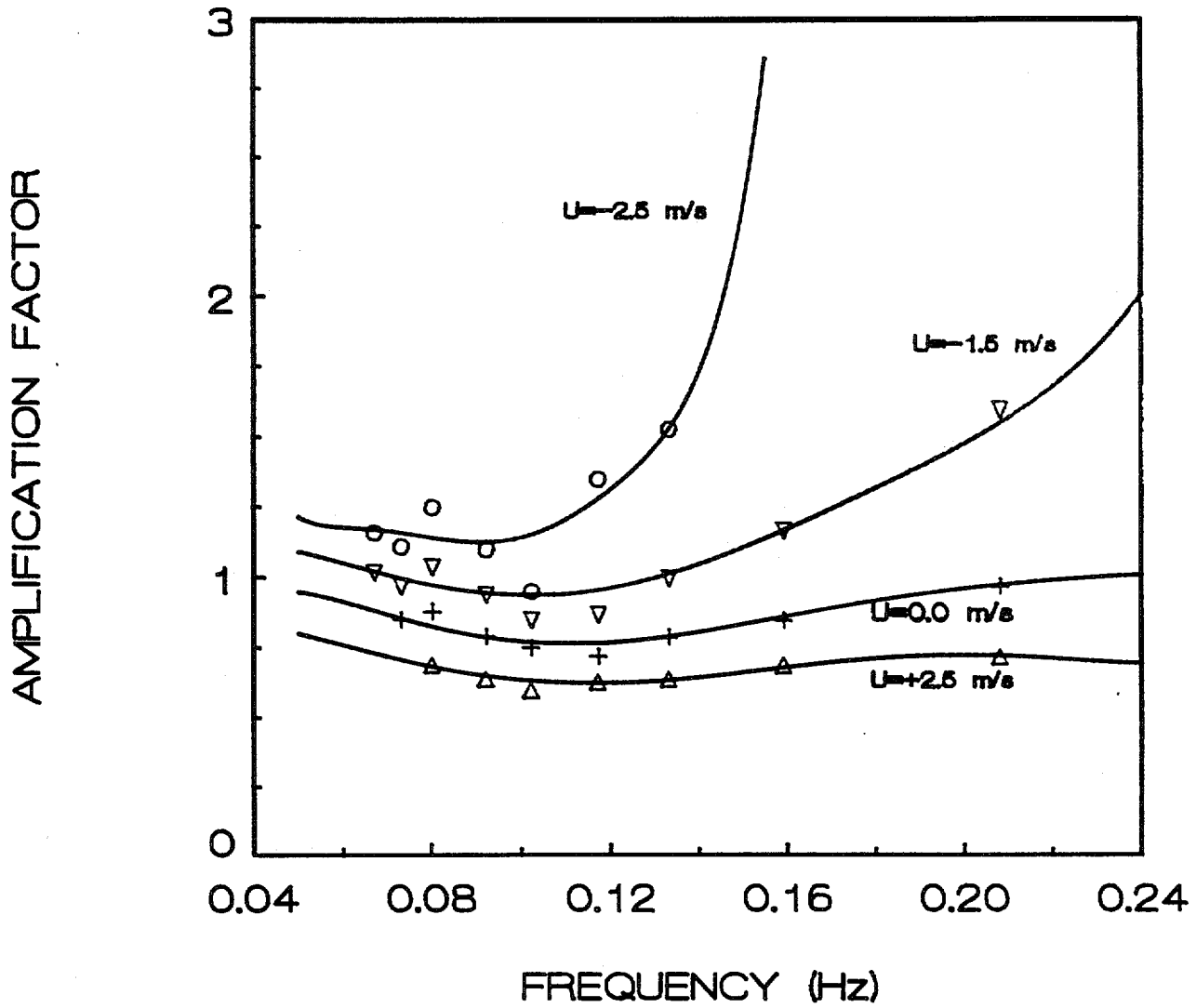COMPARISON OF ANALYTICAL & NUMERICAL
SOLUTIONS FOR INCIDENT ANGLE=60 DEGREES

Figure 6: Comparison of numerical and anlytical solutions(solid lines) of the amplification
factors for 60 degree incident wave directions.

and bottom conditions remaines to be verified.

In this model, the limiting wave spectrum is specified in a very simple manner. We modify the Wallop spectrum for water of finite depth (Huang et al.,1983) by using a breaking criterion on the significant slope of the spectrum and assume that the spectrum so obtained is the desired limiting spectrum. The predicted refracted spectrum is then compared with the limiting spectrum for each frequency band. For thoses portions of the refracted spectrum which are greater than the corresponding limiting spectrum, it is assumed that these components waves have broken and have reduced to the limiting form. The portion of spectrum beyond the cutoff frequency will always be represented by the limiting spectrum of corresponding frequency. The derivation of limiting spectrum is described below.

Based on wave dynamics of Stokes waves in the water of intermediate depth and solitary wave and cnoidal wave in shallow water, Huang et al.(1983) have proposed an ideal spectral form for waves in finite water depth. It is given by

$$\Phi(\omega) = \frac{\beta g^2}{\omega_p{}^5} \left(\frac{\omega_p}{\omega}\right)^m \exp\left[-\frac{m}{4}\left(\frac{\omega_p}{\omega}\right)^4\right] \tag{54}$$

where ω_p is the frequency at the spectral peak and β and m are functions of the significant slope, ξ, defined as

$$\xi = \frac{(\overline{\eta^2})^{1/2}}{L_p} \tag{55}$$

where $\overline{\eta^2}$ is the mean square sea surface fluctuation and L_p is the wave length connected with σ_p through the dispersion relation. The quantity β is defined as

$$\beta = \frac{m^{(m-1)/4}}{4^{(m-5)/4}} \frac{(2\pi\xi)^2}{\Gamma[(m-1)/4]}(\tanh^2 kh) \tag{56}$$

where $\Gamma[.]$ is the Gamma function.

The quantity m gives the magnitude of the slope of the line (on log-log scale) connecting the spectral peaks at σ_p and its second harmonic $2\sigma_p$. It has different expression depending upon the wave model chosen to specify the basic form of the wave field ensemble. An inportant parameter which characterize the wave profile in shallow water is the modified Ursell number which is defined, for the ensemble wave field, as

21

$$u_r = \frac{k(\overline{\eta^2})^{1/2}}{(kh)^3} = \frac{2\pi\xi}{(kh)^3} \tag{57}$$

Figure 4 of Huang et al.(1983) paper shows the variation of the spectrum slope, m, for Stokes, cnoidal and solitary wave model in terms of ξ, kh and u_r. Also shown in the figure is plots of data obtained from field and laboratory experiments by various investigators. For convenience of discussion, the cited figure is shown as Figure 7 [3]. An additional curve denoted as 'limiting spectum slope' appears in Figure 7. It is the proposed 'm' curve for computing the breaking wave spectrum in the water of finite depth. The derivation of this curve will be presented shortly.

From a theoretical point of view, the cnoidal wave model offers a general representation of the wave field because the wave profile approaches solitary wave for $kh \ll 1$ and the sinusoidal for $kh \gg 1$ which is very close to the Stokes waves. However, on the basis of the results of numerical and physical experiments as shown in Figure 5, Huang et al.(1983) have concluded that the complex expression of the m quantity for cnoidal waves (which involves the complete elliptic integral) does not provide results better than those derived from other two wave models for which the quantity m are expressed in term of the elementary functions. As a result, they have recommended that for $kh \geq 0.75$, the quantity m should be obtained from the Stokes wave model while for $kh \leq 0.75$ the solitary wave model is more appropriate.

It can be observed from Figure 5 that there exists a 'numerical' gap between the limiting line of $kh = 0.75$ on the Stokes family and the solitary wave. The gap, fortunately has been filled by data obtained from the laboratory experiment. Two set of experiments were conducted. The first set of experiments was conducted over a uniform sloping beach with the slope at 1/10, 1/15, and 1/35. The second set was conducted over a flat but movable sediment bottom. All waves were generated mechnically by a piston type paddle. It is worthwhile to note that the wave measurements were all made at the breaking point. Consequently data presented in the figure can be considered as upper limit condition. Furthermore,the effects of bottom slope and bottom material appears insignificant.

To obtain the breaking spectrum in the region $kh \geq 0.75$ we invoke the limiting steepness of simple progressive waves in shoaling water proposed by Miche(1944, see SPM 1984),

$$\frac{H_b}{L} = \frac{1}{7}\tanh kh \tag{58}$$

where $L = 2\pi/k$ is the wavelength.

For a sinusoidal wave train,

---

[3]Courtesy of Dr. N. Huang, NASA.
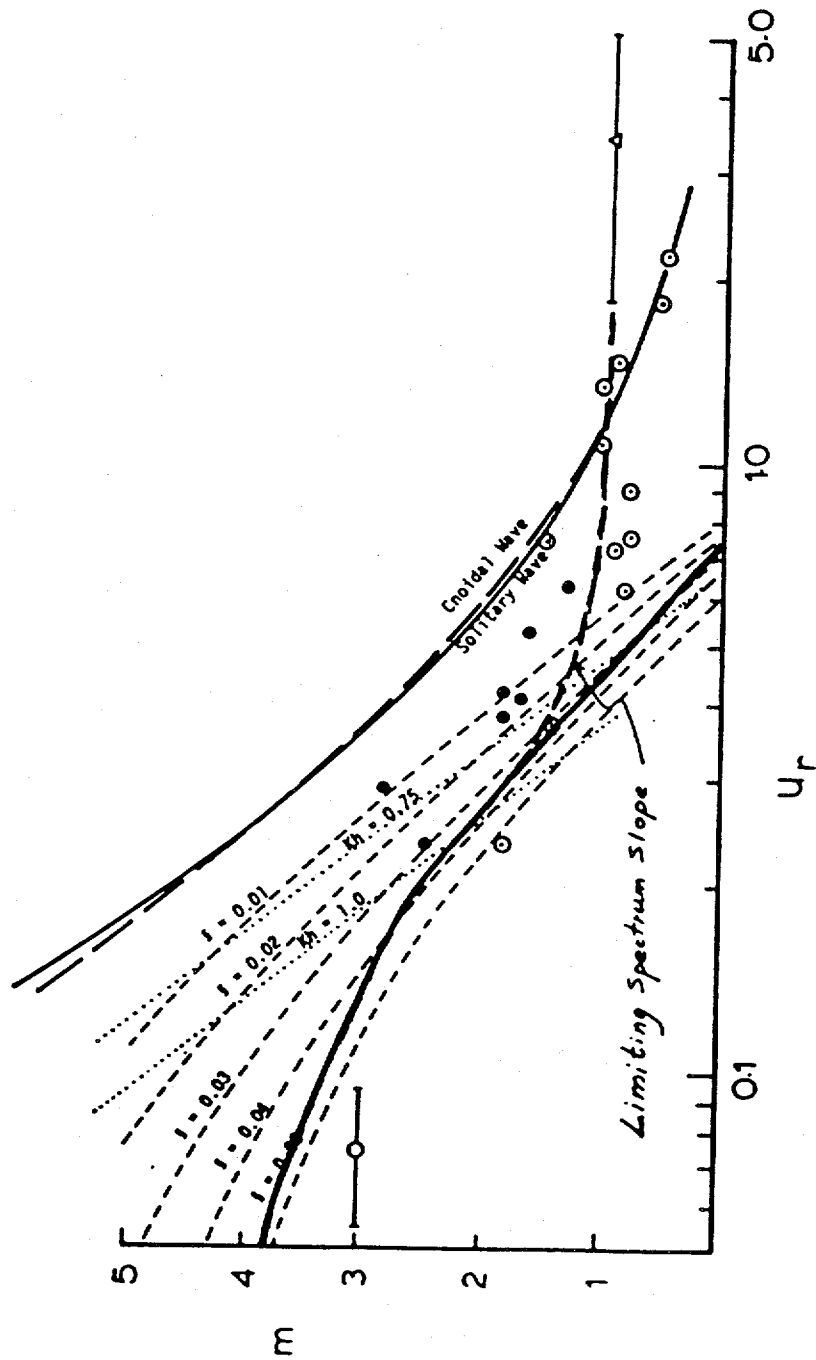
Figure 7: Variation of the spectrum slope for Stokes waves, cnoidal waves and solitary wave as function of the significant slope, relative depth and the Ursell number[after Huang et al.(1983)]

23

$$(\overline{\eta^2})^{1/2} = H/(2\sqrt{2}) \tag{59}$$

thus from Equation 55 we have

$$\xi_b = 0.0505 \tanh kh \tag{60}$$

We assume ξ_b represents the significant slope of the limiting spectrum for conditions $k_p h \geq 0.75$. and can be used to replace ξ in the original equation for m derived based on Stokes wave model to obtain,

$$m = \left| \frac{\log\{\sqrt{2}\pi\xi_b[1 + 3/(2\sinh^2 k_p h)]\coth^2 k_p h\}}{\log\sqrt{2}} \right| \tag{61}$$

The values of m computed by Equation 61 is shown in Figure 7 indicated as "limiting spectrum slop". For u_r smaller than 0.1 or so, the m value is close to the value corresponds to $\xi = 0.05$ which is the upper limit for Stokes wave in deep water. As the curve reaches $u_r = 0.3$, the corresponding ξ_b is 0.0365. After passing this point the m value becomes unrealistic in comparison with experimental data. Therefore the applicability of equation 61 is $kh \geq 0.75$ and $u_r \leq 0.3$.

To determine ξ_b for conditions $k_p h \leq 0.75$ we invoke the relationship derived by Munk(1949, or see SPF 1984) from a modified solitary wave theory. The effect of bottom slope on breaking wave condition is ignored. This relationship is simply

$$H_b = 0.78h \tag{62}$$

For solitary wave, Huang et al.(1983) have shown that

$$(\overline{\eta^2})^{1/2} = \Lambda H_b \tag{63}$$

where

$$\Lambda = \left\{ \frac{\tanh \delta}{\delta} \left[1 - \frac{1}{3}\tanh^2 \delta - \frac{\tanh \delta}{\delta} \right] \right\}^{\frac{1}{2}} \tag{64}$$

$$\delta = \pi \left(\frac{3}{4}U_r \right)^{1/2} \tag{65}$$

Hence,from equations 55 and 62, we have

24

$$\xi_b = \frac{0.78}{2\pi} k_p h \Lambda \tag{66}$$

The remainnig problem concerns with the expression for m in this relatively shallow region. A straight foreward application of Huang et al.(1983) equation derived from the solitary wave model presents some difficulty. Since an expression is needed to compute m for the gap between Stokes and solitary wave models and since field data show a simple trend of m for large u_r, the following emperical equations are used in our model:

$$m = \begin{cases} 1.83 - 0.74(\ln u_r + 1.2) & \text{if } 0.3 \le u_r \le 1.1 \\ 1.001 & \text{if } u_r > 1.1 \end{cases} \tag{67}$$

The curve denoted as 'limiting spectrum slope' in Figure 7 represents the combination of Equations 61 and 67. Once the limiting spectrum slope is determined, the quantity, β, can be computed from equation 56, and subsequently, the limiting spectrum from equation 54. We shall use this limiting spectrum as the maximum allowable spectrum when current and waves are in opposite direction. It suggests that the spectrum is not allowed to increase beyond the breaking wave limit for waves in the water of finite depth.

NUMERICAL PREDICTION PROCEDURE

The procedure of predicting wave conditions at the Columbia River entrance is sketched as given in Figure 8. Three types of input data are required to run the model. They are offshore waves spectra, refraction parameters and currents data.

Wave spectra of the source region are obtained from the OPC operational global wave forecasts for grid points $125.0°W$, $45.0°N$ and $125.0°W$, $47.5°N$. The directional spectrum has 15 frequency bands and 24 directions,ranging from azimuths $7.5°$ to $352.5°$, with an angular interval of $15°$. Forecasts are generated at 3 hour intervals.

The required refraction parameters include the amplification factor,the coordinates and direction of the ray point in the source region and time of wave propagation from that point to the forecast point in the river entrance, $124.08°W$, $46.25°N$. Each parameter is a function of the spectral frequency and directional bands, and currents at the forecast point as well. The directional bands of the spectrum to be estimated for the forecast point are coincided with those for the deep water spectrum. However, of 24 directional bands, only about 10 or so direct to the source region. Therefore, for each 15 frequency bands , wave rays are calculated for directions between azimuths $202.5°$ and $337.5°$ with
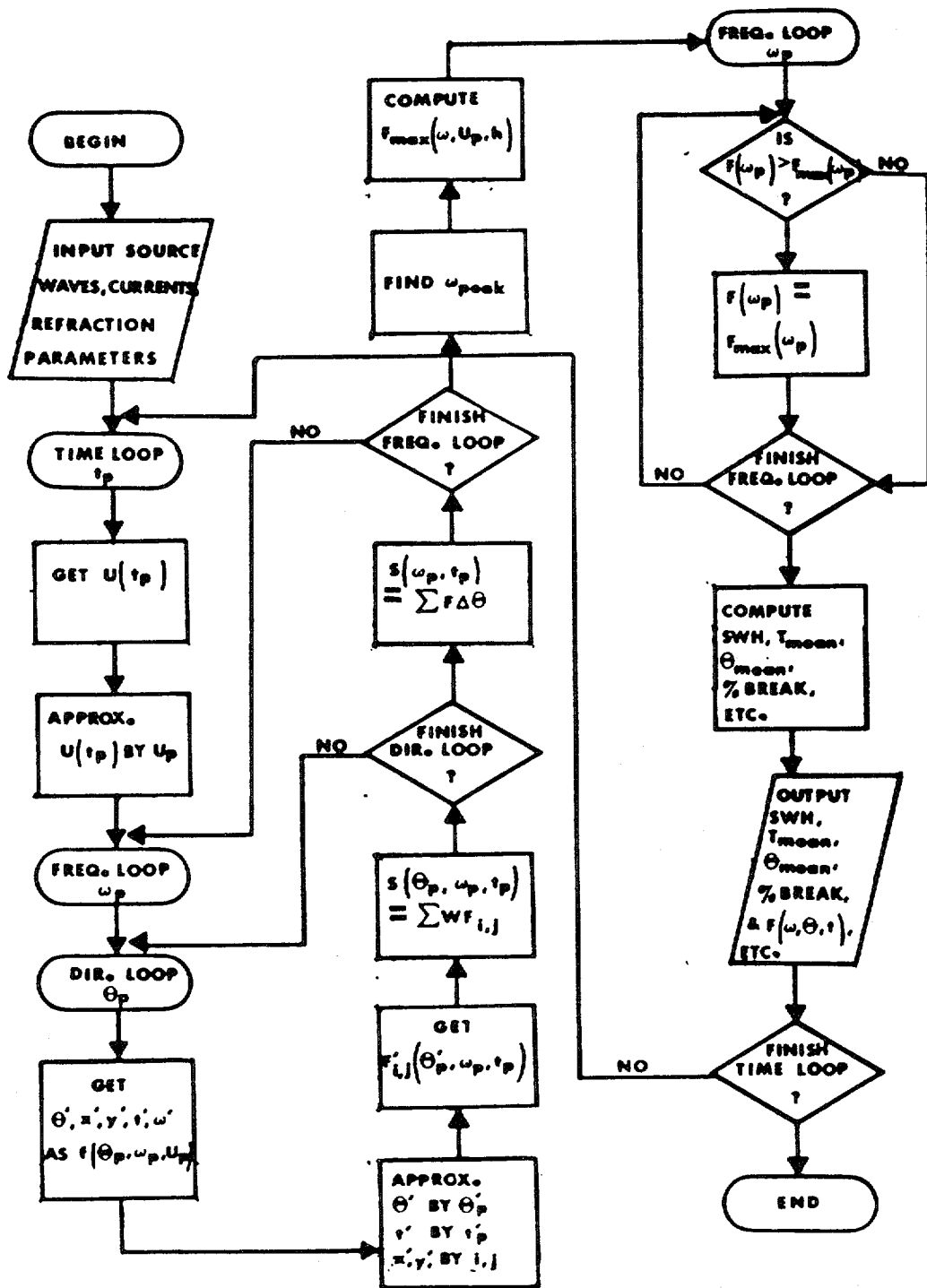
Figure 8: Procedure of numerical prediction

$\Delta\theta/2 = 7.5°$ intervals, and the currents range from -3.0 m/sec to 3.0 m/sec with an interval of 0.5 m/sec(a minus sign represents ebb current). The current distribution is assumed to be linearly decrease from the entrance to a depth of 60 meter as was assumed by Gonzalez et al.(1984). The bathymetric data used for ray calculations were obtained from the National Geophysical Data Center at 5 minutes angular intervals and covers an ocean area from $42°N$ to $48°N$ latitude and from $124°W$ to $126°W$ longitude. Figure 9 shows examples of the caluculated $\theta \sim \theta'$ curve, $|\delta\theta/\delta\theta'|$, and the amplification factor. This figure is in contrast with Figure 3 which is constructed based on linear sloping bottom. The computed results are more scattered in Figure 9 but the general patterns are similar.

In order to obtain tidal current velocity for the time at which wave prediction for the river entrance will be made, the monthly tidal current time series are pre-computed and saved in a file. The tidal current velocity at Station 695 is calculated based on the following equations [4]:

From slack to flood,

$$U_{695}(t) = F \cos\left(270. + \frac{t-s}{f-s} \times 90.\right) \tag{68}$$

From flood to slack,

$$U_{695}(t) = F \cos\left(90. - \frac{s-t}{s-f} \times 90.\right) \tag{69}$$

From slack to ebb,

$$U_{695}(t) = E \cos\left(90. + \frac{t-s}{e-s} \times 90.\right) \tag{70}$$

From ebb to slack,

$$U_{695}(t) = E \cos\left(270. + \frac{s-t}{s-e} \times 90.\right) \tag{71}$$

where E and F denote the ebb and flood current speeds, while e, f and s represent the time in minutes of ebb, flood and slack, respectively, and t is the desired time of prediction in minutes. The information regarding E, F, e, f and s can be obtained from the tidal current tables published by the NOAA/National Ocean Service for Station 695 which is about 5 km upstream from the entrance. Gonzalez et al. (1984) have made tidal current measurements near the entrance using drifter buoys during September 10 to 13, 1981. A comparison of the observed data with the estimated current velocities at Station 695, U_{695}, is given in Figure 10. The estimated values are consistently smaller than drifters speeds. Based on the regression line visually drawed, the following empirical relation is used to calculate current velocity at three hour intervals for the river entrance:

$$u(t) = 4.0 \times U_{695}(t) \tag{72}$$

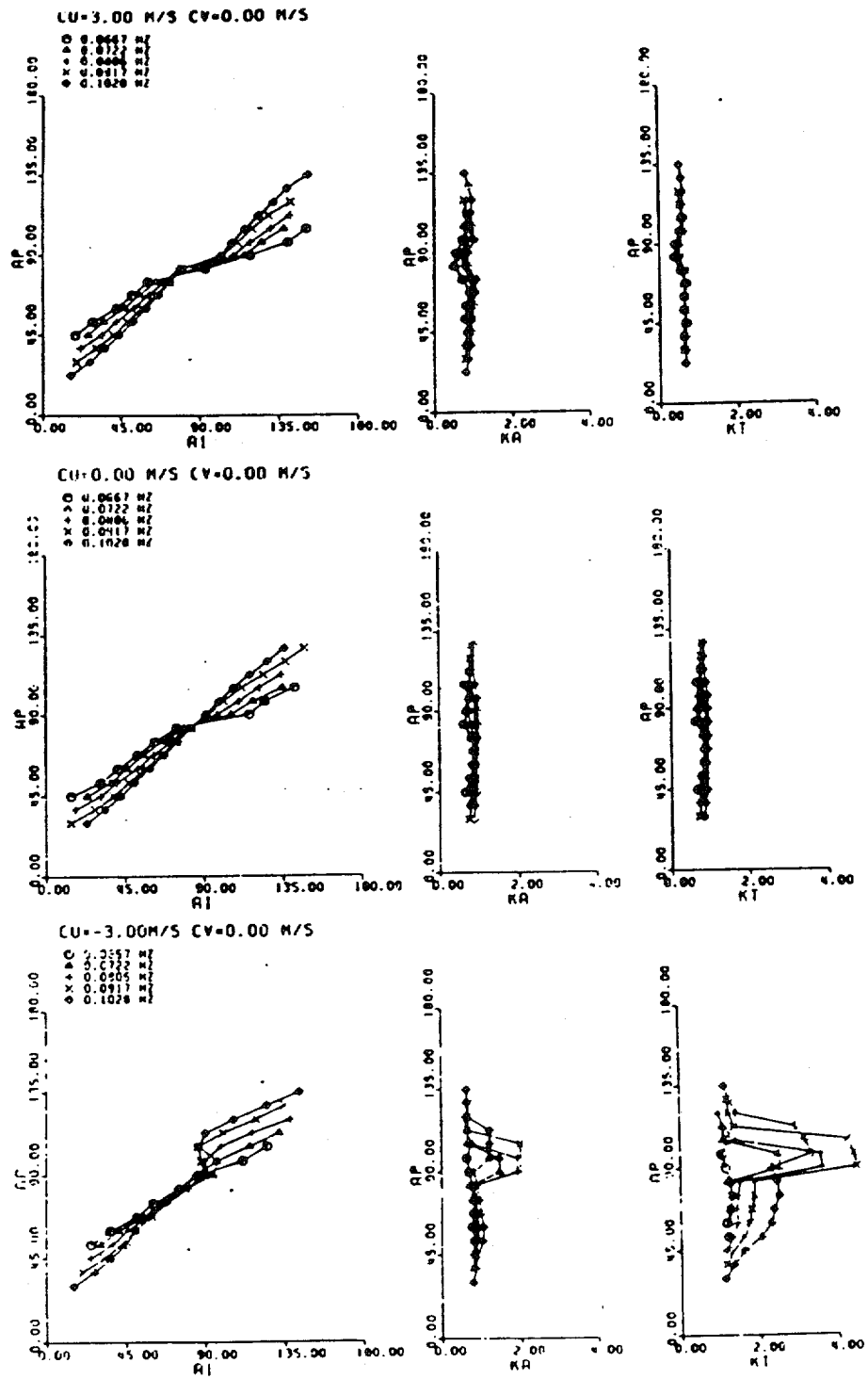[4]Courtesy of Mr. Done Simpson, NOAA/NOS

Figure 9: Same as Figure 3 except using the depth field of the Columbia River Bar area.

Monthly tidal current time series is prepared in this manner and stored in a pamanent file at 3 - hour intervals to coincide with forecast projection hours.

The next step is to determine the appropriate spectral component at source, which is considered to arrive at the forecast point at a projection time t_p, and at a specified spectral direction θ_p after undergoing refraction processes. The problem is that the directional spectrum is given in fixed discrete directional bands and projection hours. The coordinates of the end point of a ray in the source region,usually, will not be lying on a global wave grid point, the time $t_p - \Delta t$ at which the source wave information is needed is not the projection hour of forecast. And, the initial ray directions θ_p and $\theta_p \pm 7.5°$ at the forecast point are not always stay in the same direction band in the source region. This problem is treated as follows.

Assume that the direction of the end point of the ray constructed from the forecast point with a initial direction, θ_p, is represented by θ_s. The first step is to place this direction onto an appropriate directional band say, θ'_p, determined by

$$\theta'_p = Integer \left(\frac{\theta_s}{15.0} \right) \times 15. + 7.5 \tag{73}$$

Of course, θ'_p not necessarily be the same as θ_p, i.e., the same directional band. The source spectrum at the end point of the ray may be obtained from temporal and spatial interpolation of the spectral components at neighboring global grids and at neighboring projection hours. For this model, however, we have used the "region of influence" concept instead of using an interpolation scheme. The approach is as follows. Wherever the end ray point is lying within an area $\pm1.25°$ from a global grid in both latitude and longitude, the spectrum at that grid coordinates,say i, j is used to represent the value at that ray point. Similary, depending upon which projection hour the time $t_p - \Delta t$ is closer to, the spectrum of that projection hour,t'_p, is used. This approach also is applied to approximate $u(t_p)$ by u_p which is a discrete velocity value, multiple of 0.5 m/sec within ±3.0 m/sec ranges and is one of independent variables in computing refraction parameters.

We now let the source spectrum so determined be denoted by $F'_{i,j}(\omega_p, \theta'_p, t'_p)$. Also let θ'_{p-} and θ'_{p+} denote, respectively, the directions of the ray points in the source region corresponding to the initial ray direction at the forecast point $\theta_p - 7.5°$ and $\theta_p + 7.5°$. The propagation time for these rays is the same as that of the central ray, θ_p. The angles θ'_{p-}, θ'_{p+}, and θ_p may be in different directional bands. As shown in Figure 11, typical conditions will yield four possibilities which are:

$$\theta'_p - 7.5 < \theta'_{p-} < \theta'_{p+} < \theta'_p + 7.5 \tag{74}$$

$$\theta'_p - 7.5 < \theta'_{p-} < \theta'_p + 7.5 < \theta'_{p+} < \theta'_p + 22.5 \tag{75}$$

$$\theta'_p - 22.5 < \theta'_{p-} < \theta'_p - 7.5 < \theta'_{p+} < \theta'_p + 7.5 \tag{76}$$

29
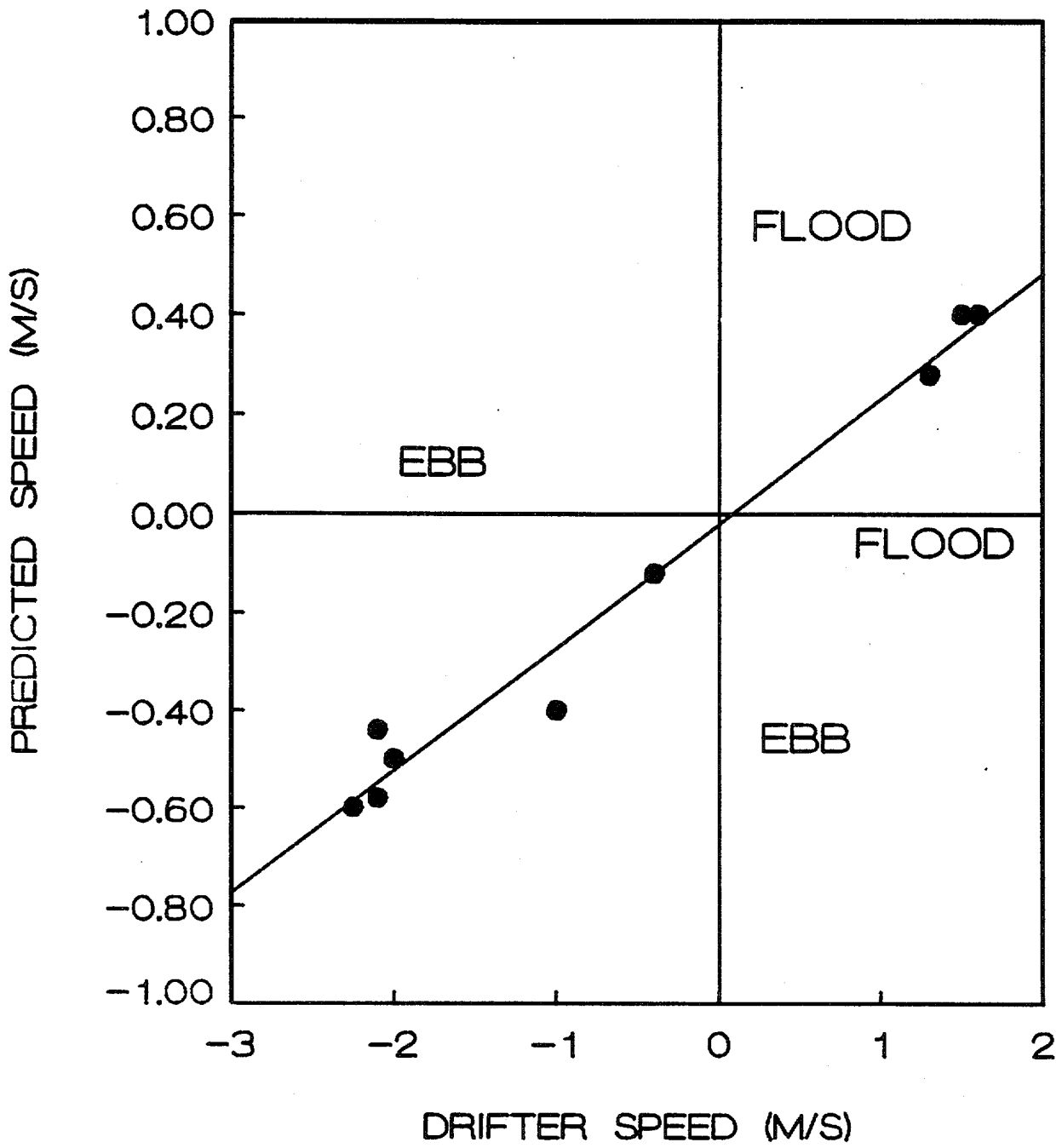
Figure 10: Comparison of predicted tidal current velocity at Station 695 and drifter velocity near the Columbia River entrance.

$$\theta'_p - 22.5 < \theta'_{p-} < \theta'_p - 7.5 < \theta'_p + 7.5 < \theta'_{p+} < \theta'_p + 22.5 \tag{77}$$

From the first possibility, the spectrum at the forecast point and at t_p is given by

$$F(\omega_p, \theta_p, t_p) = F'_{i,j}(\omega_p, \theta'_p, t'_p) \left[\frac{\theta'_{p+} - \theta'_{p-}}{15} \right] W(\omega_p, \theta_p, u_p) \tag{78}$$

From the second possibility,

$$
\begin{aligned}
F(\omega_p, \theta_p, t_p) = & \\
F'_{i,j}(\omega_p, \theta'_p, t'_p) & \left[\frac{(\theta_p + 7.5) - \theta_{p-}}{15} \right] W(\omega_p, \theta_p, u_p) \\
+ F'_{i,j}(\omega_p, \theta'_p + 15, t'_p) & \left[\frac{\theta'_{p+} - (\theta'_p + 7.5)}{15} \right] W(\omega_p, \theta_p + 7.5, u_p)
\end{aligned}
\tag{79}
$$

From the third possibility,

$$
\begin{aligned}
F(\omega_p, \theta_p, t_p) = & \\
F'_{i,j}(\omega_p, \theta'_p, t'_p) & \left[\frac{\theta_{p+} - (\theta'_p - 7.5)}{15} \right] W(\omega_p, \theta_p, u_p) \\
+ F'_{i,j}(\omega_p, \theta'_p - 15, t'_p) & \left[\frac{(\theta'_p - 7.5) - \theta_{p-}}{15} \right] W(\omega_p, \theta_p - 7.5, u_p)
\end{aligned}
\tag{80}
$$

From the fourth possibility,

$$
\begin{aligned}
F(\omega_p, \theta_p, t_p) = & \\
F'_{i,j}(\omega_p, \theta'_p - 15, t'_p) & \left[\frac{(\theta'_p - 7.5) - \theta_{p-}}{15} \right] W(\omega_p, \theta_p - 7.5, u_p) \\
+ F'_{i,j}(\omega_p, \theta'_p + 15, t'_p) & \left[\frac{\theta_{p+} - (\theta'_p + 7.5)}{15} \right] W(\omega_p, \theta_p + 7.5, u_p) \\
+ F'_{i,j}(\omega_p, \theta'_p, t'_p) & \, W(\omega_p, \theta_p, u_p)
\end{aligned}
\tag{81}
$$

For some special set of points, either $\theta_{p+} > \theta'_p + 22.5°$ or $\theta_{p-} < \theta'_p - 22.5°$ or both, could occur. The spectrum after refraction then also involves the spectra for $\theta'_p + 30°$ and $\theta'_p - 30°$ before refraction, and the number of terms in the sum may increases.

31

Figure 11: The four possible combination of θ_{p-} and θ_{p+}.
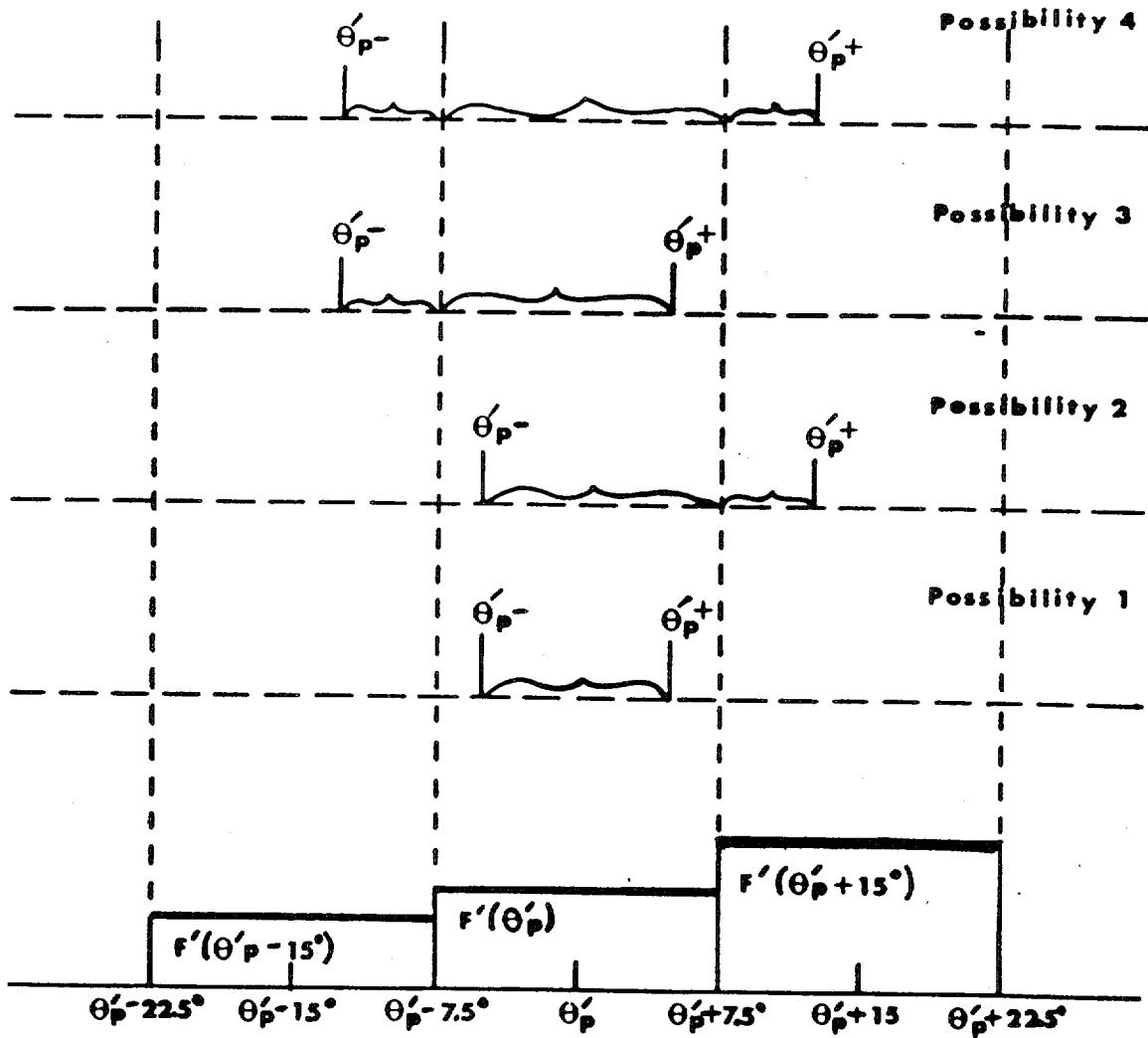
Finally, the calculated refracted wave spectrum at the forecast point is checked with the breaking wave spectrum criterion described in a previous section to ensure that the calculated frequency spectrum does not exceed the correspoinding breaking spectrum.

NUMERICAL EXPERIMENTS

Adequacy of the proposed model needs to be evaluated. However, a simultaneous measurement of both wave and current conditions in the area of interest is difficult to perform and field data are scarce. Only a limited amount of data are available. These data were obtained from a field observation program carried out during the period 10-13 September 1981 (Gonzalez et al., 1984). The offshore wave information are also available from NOAA Data Buoy Center (NDBC) routine wave measurements at two buoy locations. Buoy 46010 is located 10 km southwest of the entrance in a 60 meter water depth. Buoy 46005 is about 500 km due west of the entrance. Based on data obtained from the aforementioned measurements, the model validation tests are made for the following cases:

Table 1: Three testing cases.

Case	Wave Source	Bathymetry	Approach
(a)	Buoy 46005	Two-Dimensional	Spectral wave approach
(b)	Buoy 46010	Linear slope	Significant wave approach
(c)	Buoy 46010	Linear slope	Spectral wave approach

The first case is intended to test the full scope of the present model. The required two-dimensional source wave spectra are obtained by multiplying measured frequency spectra with the cosine-square energy spreading factor to form frequency- directional spectra. The direction of maximum energy is assumed to be coincided with the measured wind direction. This approach seem reasonable as the dominat wind direction during this period of time is westerly. In the second case, refracted waves at the river entrance are calculated by using significant wave heights and periods measured at Buoy 46010 as source waves and assuming a linear sloping bottom, the same conditions assumed by Gonzalez et al.(1984). In the third case, the spectral approach is used to calculate refracted wave heights at the river entrance while the source and bottom conditions are the same as the second case.

Figure 12 summarizes the result of calculations for these three cases in comparison with observed data. Due to sparsity of data points, it is difficult to draw a definite conclusion. Either case seems capable of providing a reasonable prediction. However, by comparing case

33

(b) and case (c) it seems that using the significant wave approach and assuming a linear sloping bottom will overpredicts the wave height at the river entrance. And by comparing case (a) and (c), it appears that the two-dimensional bottom bathymetry specification in the present model produces results as good as the simple linear slope assumption, even though the wave source for case (a) is further away from the river entrance than that of case (c). In view of the consistency of the model results with field measurements, it might be concluded that the proposed numerical modeling approach is adequate.

For real time wave forecasts of the river entrance, it is necessary to use forecasted deep water wave information. The use of buoy data to calculate refracted wave conditions at the river entrance may provide quasi 'nowcast' for forecast validation purpose but certainly cannot be used for forecast purpose. The time series of (a) offshore significant wave height forecast near the buoy station 46005 and the concurrent measurement and (b)the predicted wave height and tidal current at the river entrance are shown in Figure 13 and 14, respectively. In contrast to the slowly varying nature of offshore wave height forecast, the quasi periodic variation of the wave height at the river entrance in response to tidal variation is phenominal. Also included in Figure 14 is the concurrent forecast made independently by the Seattle marine forecasters. The forecast can be obtained through the AFOS network. Because of the descriptive nature of the Seattle forecast, only the maximum wave height and the correspoinding time of occurence can be estimateed. There is no concurrent measurement to judge which prediction is better than the other. The figure is presented only to illustrate a graphic aspect of the present model.

The idea of having local marine forecasters to operate the model any time considered appropriate has been proposed. As mentioned previously, the global wave model (the so-called NOW model) generates wave spectra forecasts daily at three-hour intervals up to 72 hours in 24 direction and 15 frequency spectral bands. However, locally available wave data through the present AFOS system are only for every 12-hours interval up to 60 hours and limited to 12 directions with an angular interval of 30 degrees while the frequency bands remain the same. A PC version of the original(mainframe) program has been developed using a 30 degrees spectral directional band for the refracted spectrum. Wave forecast can be made any time within +24 hours. A detailed description of the procedure to operate the PC version is given in the appendix.

To test the adequacy of the reduced model (PC version), a comparison is made with concurrent forecasts provides by the full version model run on the NMC NAS9000 main frame computer and the present forecasts made by the Seattle marine forecasters. Again, only the maximum wave heights are used. Figure 15 shows an intercomparison of these three types of forecasts for the Columbia River entrance. The main frame forecasts consistently yield higher wave heights than the PC and Seattle forecasts except for wave heights lower than 2 meter (6 ft) or so. On the other hand, in comparison with PC version, the Seattle forecasts yield slightly lower values for waves above 6 meters (19ft) and slightly higher for waves below 6 meters. Similar trends are shown for the two forecasts, but the seattle forecast seems to have wider scattering.

34

Figure 12: Comparisons of predicted and observed significant wave height for three tested cases. See text for explanations of these cases.
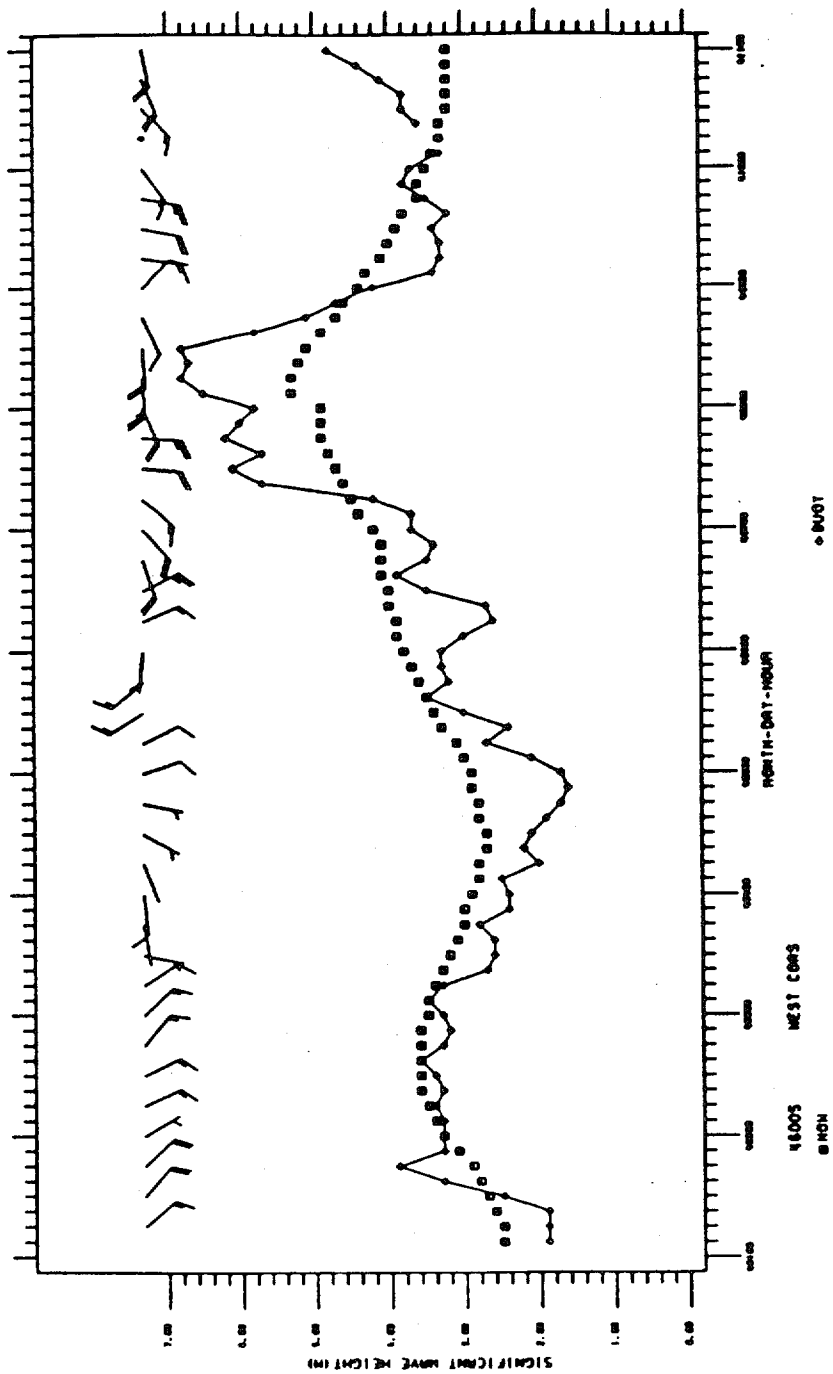
Figure 13: A time series of deep water wave heights measured at buoy station 46005 and forecasted by the global wave model (NOW) at the nearest grid.

36
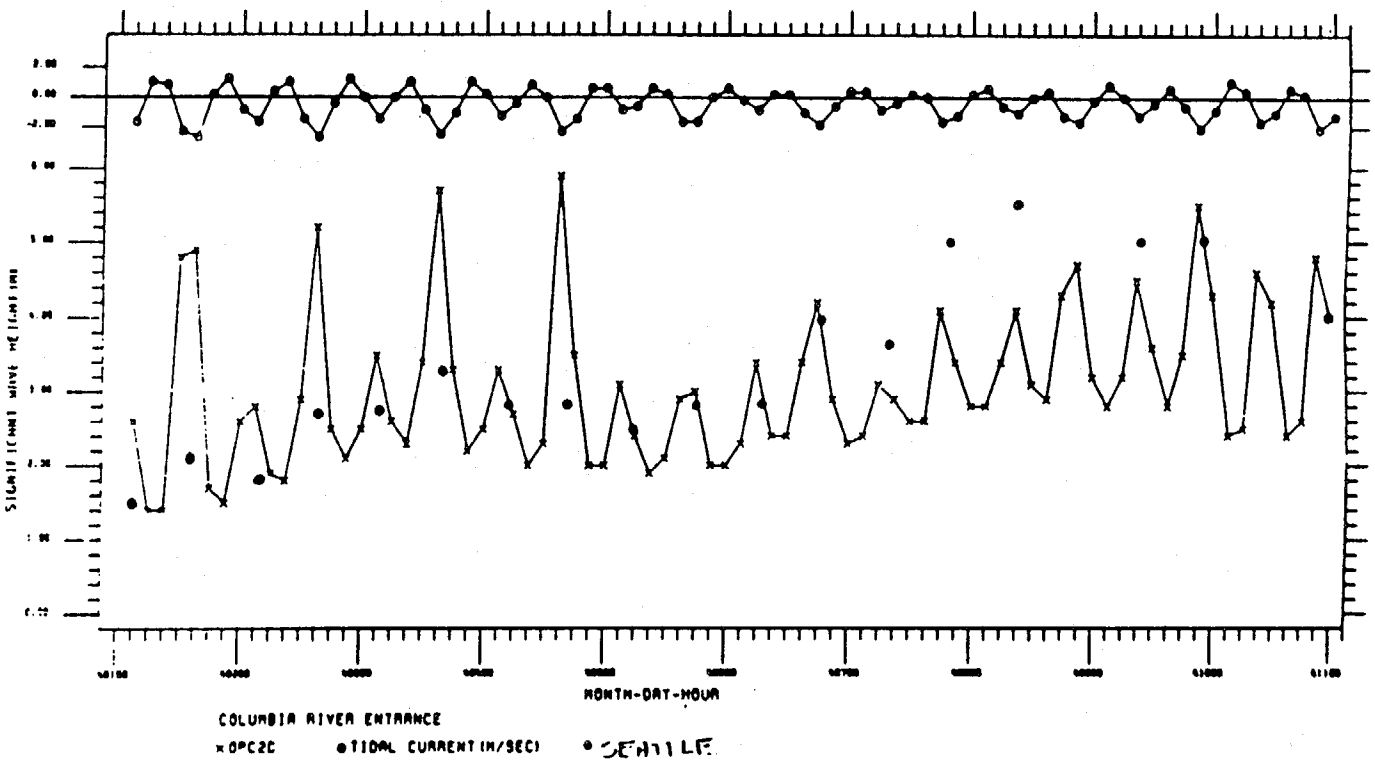
Figure 14: A time series of river entrance wave heights predicted by the present model and by the Seattle marine forecasters. Also shown is the predicted tidal currents.

37
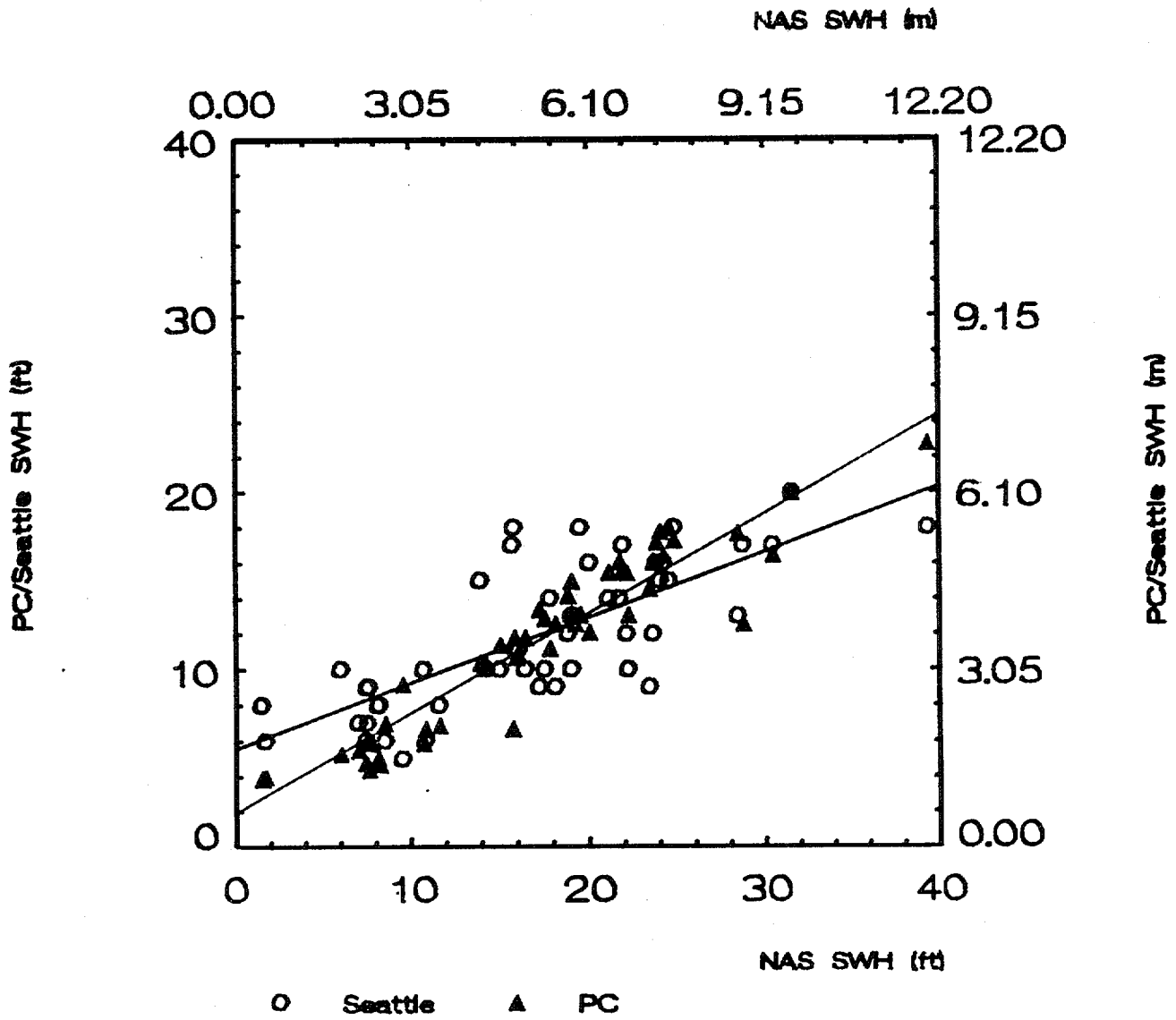
Figure 15: Comparisons of the significant wave height forecasts made by PC ,NAS main frame, and Seattle office.

It should be mentioned that the present model mainly provide results for offshore swell propagating to the river entrance. An obvious weakness of the model is on its oversimplification of the current field specification. Assumptions of unidirectional flow, without shear current(lateral variation), and a linear decrease of current speed toward offshore used in the present model are only for simplicity and convenience in calculations without rigorus justification. The grid size also is too large to specify the local bathymetric variation, such as sand bars, whose length scale is less than the grid size yet large enough to affect wave refraction substantially. Further extension of the model to incorporate local wind effects may be made. However, it is necessary to make as realistic a validation of the forecasts as possible with sufficient field data before embarking on further developments of the model.

ACKNOWLEDGEMENTS

REFERENCES

Bretherton, F. P. and C. J. Garrett (1969): Wave trains in inhomogeneous moving media. Proc. Roy.Soc. A,302,529-555.

Chao, Y. Y. (1971): An asymptotic evaluation of the wave field near a smooth caustic. J. Geophys. Res. 75(30),7401-7408.

Dorrestein, R. (1960): Simplified method of determining refraction coefficients for sea waves. J. Geophys. Res. 65(2), 637-642.

Gonzalez, F. I. (1984): A case study of wave-current- bathymetry interactions at the Columbia River entrance. J. Phy. Oceanography,14(6),1065-1078.

Gonzalez, F.I., M. R. Mulhern, E. D. Cokelet, T. C. Kaiser, J. F. Gower and J. Wallace (1984): Wave and current observations at the Columbia River entrance, 10-13 September 1981. NOAA Tech. Memo. ERL PMEL-59,231 pp.

Huang, N. E., P. A. Hwang, H. Wang, S. R. Long and L. F. Bliven (1983): A study on the spectral models for waves in finite water depth. J. Geophys.Res. 88(C14),9579-9587.

Le Méhauté, B. and J. D. Wang (1982): Wave spectrum changes on sloped beach. ASCE, 108(WW1),33-47.

Lighthill, J. (1978): Waves in Fluids. Cambridge University Press, 504 pp.

Longuet-Higgins, M. S. (1957): On the transformation of a continuous spectrum by refraction. Proc. Camb. Phil. Soc. 53(1),226-229.

Mapp, G. R., C. S. Welch and J. C. Munday (1985): Wave refraction by warm core rings. J. Geophys. Res. 90(C4),7153-7162.

Miche, M. (1944): Mouvements ondulatoires de la mer en profondeur constante ou decroissante. Annales des Ponts et Chausses, pp.25-78,131-164,270-292 and 369-406.

Munk, W. H. (1949): The solitary wave theory and its application to surf problems. Annals of the New York Academy of Sciences,Vol 51, 376-462.

Munk, W. H. and R. S. Arthur (1952): Wave intensity along a refracted ray. Gravity Waves. U.S. Nat'l Bureau of Standards, Circular 521, 95-108.

Peregrine, D. H. (1976): Interaction of water waves and currents. Aadvance in Applied Mechanics, Vol.16,10-117.

Phillips, O. M. (1977): The Dynamics of the Upper Ocean. Cambridge University Press, 336 pp.

Pierson, W. J., Jr. (1950): The interpretation of crossed orthogonals in wave refraction phenomena. TM-21, US Army,Corps of Engineers, Beach Erosion Board.

Pierson, W. J., Jr., J. J. Tuttell and J. A. Woolley (1953): The theory of the refraction of a short crested Gaussian sea surface with application to the northern New Jersey coast. Proc. 3rd Conf. on Coastal Eng.,86-108.

Shen, M. C. and J. B. Keller (1975): Uniform ray theory of surface,internal and acoustic wave propagation in a rotating ocean or atmosphere. SIAM J. Appl. Math. 28(4),857-875.

Skovgaard, O. and I. G. Jonsson (1976): Current depth refraction using finite elements. Proc. 15th Conf. on Coastal Eng. (1)721-737.

SPM (1984): Shore Protection Manual, Vol I, Coastal Engineering Research Center, US Army Corps of Engineers.

Tung, C. C. and N. E. Huang (1987): Breaking wave spectrum in water of finite depth in the presence of current. Tech. Rept. CERC-87-19, US Army Corps of Engineers, 28 pp.

APPENDIX

COLUMBIA RIVER BAR WAVE FORECAST PROGRAM – PC VERSION
INSTRUCTION MANUAL

PURPOSE

This program forecasts the transformation of offshore waves at the Columbia River Bar under the influence of bottom topography and tidal currents. The forecast generated for the Columbia River Bar displays the significant wave height, wave direction, mean wave period, peak wave period and likelihood of breakers(in %) at the user specified time(within 24 hr.). The offshore wave forecast, which provides input wave data for the bar forecast, is also displayed in terms of the latitude/longitude of grid points, and the significant wave height, wind speed, and wind direction for each point.

Executable programs and the input data files are provided on the enclosed floppy diskettes. A brief description of input/output data file manipulation and the forecast operational procedure is given below.

INPUT/OUTPUT FILES

AFOS WAVE SPECTRA DATA

Each day, the user must download offshore wave spectra data, generated by the NOAA Global Wave Model(NOW Model), from the AFOS system. Four AFOS messages, which correspond to two grid points at time +12 and +24 GMT, are downloaded. These grid points, identification numbers NMCOSWSP1(47.5 N, 125.0 W) and NMCOSWSP2 (45.0 N,125.0 W), are closest to the Columbia River Bar.

The procedure used to download this data is as follows:

1. Set up the PC with the software necessary for obtaining AFOS data. We used the AFOS ABT Operational Software diskette to download AFOS data onto a blank diskette.

2. On the AFOS terminal, type in the identification number for the first grid point, NFDOSWSP1 (in our case, NFDOSWSP1 was used in place of NMCOSWSP1 to call up message). The wave spectra message for that grid point at time +60(TAU 60) should appear on the screen. Press the 'Previous Version' key until TAU 24 is on the screen.[1] Type in the command ACOMMS:XMIT 2 and Enter(Note: the 2 in this command is the number of the port which ties the PC to the AFOS system; this number will differ with each setup). A

---

[1]The present version is set up to forecast up to +24 hr.

message will appear on the AFOS screen, 'Default Product Cued For Xmit', and the message will be transferred to the PC and downloaded onto the diskette. If you check the diskette, this message has been downloaded under the name NMCOSW.SP1. The identification number for the grid point is downloaded as the name of the file on the PC with a period between the sixth and seventh characters. Each downloaded message,i.e. time +12, for this grid point will be downloaded under this same name(NMCOSW.SP1). For this reason, rename the first file you download from the first grid point for +24, i.e. rename NMCOSW.SP1 to NMCOSW.SPA. The PC/DOS command for renaming files is REN NMCOSW.SP1 NMCOSW.SPA. Now, press the key 'Previous Version' on the AFOS computer console and the wave spectra for the first grid point, time +12, will appear on the AFOS screen. Again, type in the command ACOMMS:XMIT 2 and Enter. This second message will be downloaded onto the PC under the name NMCOSW.SP1. If you had not renamed the first file, the second would have over-written it. No other messages will be downloaded for this grid point so there is no need to rename this second file.

3. Follow procedure #2 to download the two messages for the second grid point. For example, the two files on the PC for this grid point (TAU 12, TAU 24) will NMCOSW.SPB and NMCOSW.SP2.

When the diskette with the 4 AFOS messages is obtained, you will combine these messages into one data file entitled 'AFOS.DAT'. For example, the four AFOS files on your diskette will be:

(1) NMCOSW.SPA TAU 24 (LAT 47.5 N, LONG 125.0 W - Time +24)
(2) NMCOSW.SP1 TAU 12 (LAT 47.5 N, LONG 125.0 W - Time +12)
(3) NMCOSW.SPB TAU 24 (LAT 45.0 N, LONG 125.0 W - Time +24)
(4) NMCOSW.SP2 TAU 12 (LAT 45.0 N, LONG 125.0 W - Time +12)

The command in PC DOS to append all of these messages into one file is:
COPY NMCOSW.SPA+NMCOSW.SP1+NMCOSW.SPB+NMCOSW.SP2 AFOS.DAT
This new data file, 'AFOS.DAT', will be read by the main program. A SAMPLE PRINTOUT OF THIS DATA FILE FORMAT IS INCLUDED WITH THIS MANUAL IN Illustration 1. It does not matter in which order the data files are appended to create AFOS.DAT.

The main program will now read the data in AFOS.DAT and load the information into memory. The program is designed to run with two day's worth of wave spectra data. The data from the previous day is stored in a data file called ISPECTRA.DAT. If this is the first run, there will only be one day's worth of AFOS data and no forecast may be made before 1300 GMT. For more information, see the section 'BEGIN OPERATIONS'.

REFRACTION PARAMETERS DATA

The refraction parameters data file (REFPARA.DAT) is a numerical data file which provides amplification factors as a function of wave frequency, direction and current speed, taking into account the two-dimensional variation of coastal bottom topography in the vicinity of the

Columbia River Bar. This is a fixed data file which the user does not change or edit. It is read by the main program.

TIDAL CURRENT DATA

A question will be put to the user - 'DO YOU WANT TO INPUT TIDAL CURRENT DATA AND THE ASSOCIATED DATE AND TIME? (YES=1, NO=2)'. It is recommended that you input the tidal current speed with the time of the forecast(ENTER 1). However, a Tidal Current Program is available which will calculate the tidal current speed for the input time of forecast(ENTER 2). For information on the Tidal Current Program see the section entitled Tidal Current Program. The user, regardless of how he/she decides to calculate tidal current data, will always have to input the date and time of the forecast.

TIDAL CURRENT PROGRAM

The Tidal Current Program is run separately from the main program. This program, TID-CUR.EXE, utilizes 3 input data files to create a Tidal Current Table for the Columbia River at 3-hr intervals. This Tidal Current Table is read by the main program. The input files are TIDALR.DAT, TIDREF.DAT and TIDALC.DAT. The output file is TIDWRI.DAT. Each month the user will have to edit TIDALC.DAT by typing a month's worth of tidal current data from The Tidal Current Tables, Pacific Coast Of North America And Asia, Table 1: Daily Current Predictions, Grays Harbor Entrance, Washington. A sample printout of the format is enclosed as Illustration 2. Note that an ebb current is typed with a negative sign. It is recommended that the last day of the previous month and the first 2 days of the next month be included. The input data file TIDALR.DAT must also be edited (See Illustration 3). The user should change the third number which indicates the total number of lines in the edited data file, TIDALC.DAT. This number may change when the user edits this data file, TIDALC. DAT each month. The total number of lines in TIDALC.DAT should not exceed 65. The first number of TIDREF.DAT (See Illustration 4) is the time difference between UTC and PST. During Daylight Savings Time this number must be 7. For the rest of the year it will be 8. The user must edit this. When TIDCUR.EXE is run, the Tidal Current Table stored in TIDWRI.DAT (Input data file for the main program) is updated for the current month and may be read by the main program.

BEGIN OPERATIONS

BEFORE THE FIRST RUN:

1) The main program(COLRIV.EXE) and the input data files are on the floppy diskettes. All programs and data files should be copied into the same directory on a PC with a hard disk.

2) On the day of the first run, the user should download the AFOS Offshore Wave Spectra Data for that date onto a floppy diskette (See Input/Output Section - AFOS WAVE SPECTRA DATA - for the procedure). AFOS.DAT should then be downloaded into the directory on the hard disk of the PC in which the COLRIV.EXE and data files are stored. On the day of the first run, the user will only have one day's worth of offshore wave spectra data as opposed to

two days.

3) If the user wishes to use the Tidal Current Program to calculate tidal current data, instead of inputting the data, then see Input/Output Section - TIDAL CURRENT PROGRAM - for the procedure.

FORECAST RUNS

When the user begins the first run a series of questions will appear on the screen. The user will input the requested information.

The following synopsis is a sample of the first run the user will make:

Type COLRIV.EXE (ENTER) to run the executable program.

DO YOU WANT TO INPUT TIDAL CURRENT DATA AND THE ASSOCIATED DATE AND TIME? (YES=1, NO=2)

If the user inputs 1 and ENTER -

PLEASE TYPE IN DATE AND TIME AS YYMMDDHH (INTEGER) AND CURRENT SPEED IN KNOTS. IF EBB MAKE SPEED NEGATIVE.

88113018 -1.6 (For example, the user inputted the current day's date - November 30, 1988 and 1800 UTC for the time of the forecast. The tidal current speed was ebb so a negative sign was typed before the tidal current speed of 1.6. Also note that since this is the first run, a forecast cannot be made before 1300 UTC.) (ENTER)

The program will now begin to read data files and do calculations to print out the forecast on the screen.

If the user inputs 2 and ENTER for the first question -

PLEASE TYPE IN DATE AND DESIRED TIME OF FORECAST.
FORMAT: YYMMDDHH (INTEGER)

88113018 (For example, the user inputted the current day's date - November 30, 1988 and 1800 UTC for the time of the cast. The user chose to utilize the pre-calculated forecast. The user chose to utilize the precalculated Tidal Current Table so no tidal current speed is inputted manually.) ENTER

The program will now begin to read data files and do calculations to print out the forecast on the screen.

After the forecast for the user specified date and time has been written to the screen, the following question will appear:

DO YOU WANT TO MAKE ANOTHER FORECAST FOR A DIFFERENT TIME? (YES=1, NO=2)

If the user inputs 1 (ENTER) then the first question will appear on the screen again: DO YOU WANT TO INPUT TIDAL CURRENT DATA AND THE ASSOCIATED DATE AND TIME? (YES=1, NO=2)

The same process will begin again. This time the run time will be faster because the refraction parameters (REFPARA.DAT) have already been read into memory, and this file will not be read again while the program is running. Note that the user has the choice of iputting the tidal current data or using the Tidal Current Program for the second forecast, regardless of the choice made for the first forecast. Just make sure that the Tidal Current Program has been run prior to the execution of the main program. When the forecast is written to the screen, then this question will again appear on the screen: DO YOU WANT TO MAKE ANOTHER FORECAST FOR A DIFFERENT TIME? (YES=1, NO=2) If the user wishes to exit the program, he/she will input 2 (ENTER), and the AFOS data will be stored in ISPECTRA.DAT. The following day the forecast will utilize two consecutive day's worth of AFOS data.

IMPORTANT!!!!! —— Each day, the AFOS system stores an offshore wave spectra forecast message for time +12 and +24. For the first run of this program, the user will make a data file - AFOS.DAT - for the current day. The user will be running the program with one day's worth of AFOS data instead of two. Therefore, a forecast cannot be made for a time before 1300 UTC. The program reads the AFOS data, stores it in memory, and writes it to a file called ISPECTRA.DAT. This is done when the program is terminated via the above question: DO YOU WANT TO MAKE ANOTHER FORECAST FOR A DIFFERENT TIME? (YES=1, NO=2). This file is overwritten each time the user exits the program via the normal exit. If the user wants to run the program at a later time that same day, he/she will have the AFOS.DAT file but will no longer have the previous day's data in ISPECTRA.DAT. The easiest way to circumvent this is to exit the program via the PC command ctrl-break after the first run of the program. This will break all contact with the program and the ISPECTRA.DAT (previous day's data) will not be overwritten. WARNING: Be sure to exit the program normally when all forecasts have been made for that day so that ISPECTRA.DAT will be updated for the next day. When the program is run with two day's worth of data, the user can obtain a forecast for anytime that day.

If the user has skipped a day in running the program, and has not downloaded AFOS data for that skipped day, the program will have to be run with only one day's worth of data on the next run.

[END]

ILLUSTRATION 1

AFOS.DAT

```
>##<A<
<ZCZC NMCOSWSP1
FZPZ41 KWBC 050300
```

89050300	LAT 47.5N LON 125.0W 00Z 3 MAY 89 TAU 24							
NOAA	DIR(FROM).		-LOCAL	WIND	327.2DEG	6.5KTS		
PERIOD(TOTAL)	135	165	195	225	255	285	315	345
22.5	3	0	1	1	0	0	0	0	0
20.0	17	0	5	6	4	1	1	0	0
18.0	30	1	9	10	7	2	1	0	0
16.4	37	0	11	13	8	2	2	0	0
15.0	46	0	11	19	8	3	5	1	0
13.9	58	0	6	28	8	4	10	3	0
12.4	123	0	5	58	11	7	31	10	1
10.9	91	0	2	30	5	10	35	10	1
9.7	72	0	1	26	5	9	24	6	0
8.6	70	0	0	25	12	13	17	3	0
7.5	35	0	0	12	7	8	6	1	0
6.3	23	0	0	9	6	4	2	1	0
4.8	10	0	0	3	4	2	0	1	1
3.2	7	0	0	4	1	0	0	0	0
DIR(TOTAL)		1	52	246	86	64	133	37	3
SIG HT	10.4FT								

```
NNNN
>##<A<
<ZCZC NMCOSWSP1
FZPZ41 KWBC 050300
```

89050300	LAT 47.5N LON 125.0W 00Z 3 MAY 89 TAU 12							
NOAA	DIR(FROM).		-LOCAL	WIND	8.1DEG	6.4KTS		
PERIOD(TOTAL)	165	195	225	255	285	315	345
22.5	4	1	1	1	0	0	0	0
20.0	17	5	6	4	1	0	0	0
18.0	25	7	9	6	2	1	0	0
16.4	32	8	12	7	2	3	1	0
15.0	50	6	19	6	4	11	3	0
13.9	69	4	28	7	5	19	5	0
12.4	141	3	54	10	11	48	15	1
10.9	92	1	27	4	11	38	10	1
9.7	67	1	27	5	9	20	5	0
8.6	64	0	25	11	11	13	3	0
7.5	32	0	12	7	6	5	1	0
6.3	23	0	9	7	4	1	1	0
4.8	9	0	3	3	1	0	0	0
3.2	8	0	4	2	0	0	0	0
DIR(TOTAL)		38	236	81	68	159	45	3
SIG HT	10.4FT							

ILLUSTRATION 1 (CONT.)

AFOS.DAT

NNNN
>##<A<
<ZCZC NMCOSWSP2
FZPZ42 KWBC 050300

89050300 LAT 45.0N LON 125.0W 00Z 3 MAY 89 TAU 24

NOAA   DIR(FROM).   -LOCAL WIND 349.2DEG 6.4KTS

PERIOD(TOTAL)		135	165	195	225	255	285	315	345
22.5	3	0	1	1	0	0	0	0	0
20.0	17	0	5	6	4	1	1	0	0
18.0	33	1	10	11	8	2	1	1	0
16.4	43	0	15	14	8	2	2	1	0
15.0	54	0	15	19	8	2	7	3	0
13.9	65	0	9	27	8	3	13	5	0
12.4	130	0	7	59	11	4	32	16	1
10.9	107	0	3	32	5	7	42	16	1
9.7	75	0	1	26	5	7	26	9	0
8.6	72	0	1	25	12	11	18	5	0
7.5	37	0	0	13	8	7	7	2	0
6.3	27	0	0	10	7	6	2	1	0
4.8	12	0	0	4	4	3	0	1	1
3.2	6	0	0	3	1	0	0	0	0
DIR(TOTAL)		1	69	250	92	56	150	59	5

SIG HT 10.8FT

NNNN
>##<A<
<ZCZC NMCOSWSP2
FZPZ42 KWBC 050300

89050300 LAT 45.0N LON 125.0W 00Z 3 MAY 89 TAU 12

NOAA   DIR(FROM).   -LOCAL WIND 49.9DEG 2.6KTS

PERIOD(TOTAL)		135	165	195	225	255	285	315	345
22.5	4	0	1	1	1	0	0	0	0
20.0	18	0	6	6	4	1	0	0	0
18.0	29	1	10	10	7	2	1	0	0
16.4	38	0	11	12	7	2	4	1	0
15.0	60	0	9	19	7	3	15	6	1
13.9	78	0	6	28	8	3	23	10	1
12.4	150	0	5	57	11	6	48	23	2
10.9	99	0	2	28	5	7	41	16	1
9.7	67	0	1	27	5	6	20	7	0
8.6	65	0	0	25	11	10	14	4	0
7.5	34	0	0	12	7	7	5	1	0
6.3	26	0	0	9	8	7	2	1	0
4.8	12	0	0	3	5	3	0	0	0
3.2	7	0	0	4	2	0	0	0	0
DIR(TOTAL)		1	52	242	87	57	173	69	5

SIG HT 10.9FT

ILLUSTRATION 2

TIDALC.DAT

```
8904261204  0.0 8904261441  1.8 8904261833  0.0 8904262058  -1.4
8904262354  0.0 8904270217  1.3 8904270504  0.0 8904270910  -2.9
8904271258  0.0 8904271539  1.7 8904271932  0.0 8904272212  -1.4
8904280103  0.0 8904280320  1.1 8904280611  0.0 8904281015  -2.7
8904281358  0.0 8904281650  1.7 8904282033  0.0 8904282336  -1.6
8904290222  0.0 8904290437  1.0 8904290742  0.0 8904291134  -2.6
8904291459  0.0 8904291805  1.8 8904292129  0.0 8904300045  -2.0
8904300342  0.0 8904300615  1.1 8904300912  0.0 8904301250  -2.6
8904301557  0.0 8904301916  2.0 8904302220  0.0 8905010141  -2.6
8905010452  0.0 8905010749  1.5 8905011030  0.0 8905011355  -2.7
8905011652  0.0 8905012011  2.3 8905012307  0.0 8905020234  -3.3
8905020550  0.0 8905020859  2.0 8905021139  0.0 8905021450  -2.8
8905021743  0.0 8905022053  2.5 8905022351  0.0 8905030323  -3.8
8905030643  0.0 8905030954  2.5 8905031240  0.0 8905031544  -2.8
8905031831  0.0 8905032138  2.6 8905040034  0.0 8905040407  -4.3
8905040731  0.0 8905041043  2.8 8905041337  0.0 8905041633  -2.8
8905041917  0.0 8905042219  2.6 8905050116  0.0 8905050455  -4.5
8905050819  0.0 8905051132  3.0 8905051430  0.0 8905051721  -2.7
8905052002  0.0 8905052300  2.6 8905060158  0.0 8905060538  -4.6
8905060906  0.0 8905061217  3.0 8905061521  0.0 8905061810  -2.5
8905062047  0.0 8905062342  2.4 8905070241  0.0 8905070623  -4.4
8905070953  0.0 8905071305  2.8 8905071611  0.0 8905071859  -2.2
8905072134  0.0 8905080024  2.1 8905080324  0.0 8905080711  -4.1
8905081041  0.0 8905081356  2.5 8905081702  0.0 8905081950  -2.0
8905082223  0.0 8905090106  1.8 8905090409  0.0 8905090757  -3.7
8905091131  0.0 8905091451  2.2 8905091755  0.0 8905092045  -1.7
8905092319  0.0 8905100153  1.4 8905100458  0.0 8905100850  -3.2
8905101223  0.0 8905101556  1.9 8905101849  0.0 8905102144  -1.6
8905110024  0.0 8905110252  1.0 8905110552  0.0 8905110950  -2.8
8905111317  0.0 8905111702  1.7 8905111945  0.0 8905112246  -1.6
8905120143  0.0 8905120421  0.7 8905120656  0.0 8905121053  -2.4
8905121412  0.0 8905121803  1.6 8905122039  0.0 8905122349  -1.7
8905130313  0.0 8905130622  0.7 8905130808  0.0 8905131155  -2.1
8905131506  0.0 8905131900  1.6 8905132128  0.0 8905140045  -2.0
8905140431  0.0 8905140732  0.9 8905140922  0.0 8905141254  -2.0
8905141557  0.0 8905141945  1.6 8905142213  0.0 8905150138  -2.3
8905150527  0.0 8905150831  1.2 8905151030  0.0 8905151349  -1.9
8905151644  0.0 8905152028  1.7 8905152253  0.0 8905160227  -2.7
8905160609  0.0 8905160916  1.4 8905161130  0.0 8905161437  -1.9
8905161726  0.0 8905162103  1.7 8905162330  0.0 8905170308  -3.0
8905170645  0.0 8905171001  1.7 8905171223  0.0 8905171524  -1.9
8905171805  0.0 8905172129  1.7 8905180005  0.0 8905180347  -3.2
8905180718  0.0 8905181038  1.9 8905181311  0.0 8905181607  -1.9
8905181843  0.0 8905182145  1.7 8905190038  0.0 8905190422  -3.4
8905190750  0.0 8905191111  2.0 8905191354  0.0 8905191648  -1.9
8905191920  0.0 8905192210  1.7 8905200110  0.0 8905200455  -3.6
8905200824  0.0 8905201137  2.1 8905201436  0.0 8905201724  -1.8
8905201956  0.0 8905202238  1.7 8905210141  0.0 8905210528  -3.6
8905210858  0.0 8905211204  2.2 8905211518  0.0 8905211801  -1.8
8905212034  0.0 8905212309  1.7 8905220212  0.0 8905220601  -3.7
8905220935  0.0 8905221233  2.2 8905221600  0.0 8905221836  -1.7
8905222114  0.0 8905222345  1.7 8905230245  0.0 8905230634  -3.6
8905231015  0.0 8905231308  2.2 8905231643  0.0 8905231915  -1.7
8905232158  0.0 8905240028  1.6 8905240323  0.0 8905240715  -3.5
8905241057  0.0 8905241348  2.2 8905241729  0.0 8905242003  -1.7
8905242250  0.0 8905250115  1.5 8905250407  0.0 8905250800  -3.4
8905251143  0.0 8905251433  2.1 8905251817  0.0 8905252057  -1.7
8905252349  0.0 8905260206  1.4 8905260501  0.0 8905260855  -3.1
8905261231  0.0 8905261526  2.1 8905261907  0.0 8905262201  -1.9
8905270058  0.0 8905270315  1.2 8905270610  0.0 8905270955  -2.8
```

89=YEAR	89=YEAR	89=YEAR	89=YEAR
05=MONTH	05=MONTH	05=MONTH	05=MONTH
27=DAY	27=DAY	27=DAY	27=DAY
0058=TIME OF SLACK WATER	0315=TIME OF MAX. CURRENT (FLOOD)	0610=TIME OF SLACK WATER	0955=TIME OF MAX. CURRENT (EBB)
0.0=SPEED IN KNOTS, SLACK WATER ALWAYS = 0.0	1.2=SPEED IN KNOTS	0.0=SPEED IN KNOTS, SLACK WATER ALWAYS = 0.0	-2.8=SPEED IN KNOTS. MAX. EBB CURRENT MARKED WITH A MINUS SIGN.

SEE: TIDAL CURRENT TABLES 1989/PACIFIC COAST OF NORTH AMERICA AND ASIA
GRAYS HARBOR ENTRANCE, WASHINGTON 1989

ILLUSTRATION 3

TIDALR.DAT

GRAYS HARBOR ENT.   SUB-STATION # 695   60   3

Number of lines in TIDALC.DAT. Each time
TIDALC.DAT is updated, and before the TIDAL
CURRENT PROGRAM(TIDCUR.FOR) is run, change
this value to equal the number of lines in
TIDALC.DAT. This value should not exceed
65.

ILLUSTRATION 4

8.   18. -25. -16. -32.   .3   .4

Number of hours to change from PST to UTC. During Daylight Savings Time, this
number should be updated by the user to 7.

No. 15.   Gemmill, W.H., T.W. Yu, and D.M. Feit 1987:   Performance
          Statistics of Techniques Used to Determine Ocean Surface Winds.
          Conference Preprint, Workshop Proceedings AES/CMOS 2nd Workshop
          of Operational Meteorology. Halifax, Nova Scotia.

No. 16.   Yu, T.W., 1988:   A Method for Determining Equivalent Depths of
          the Atmospheric Boundary Layer Over the Oceans. Journal of
          Geophysical Research. Vol. 93, No. C4, pp3655-3661.

No. 17.   Yu, T.W., 1987:   Analysis of the Atmospheric Mixed Layer Heights
          Over the Oceans. Conference Preprint, Workshop Proceedings
          AES/CMOS 2nd Workshop of Operational Meteorology, Halifax, Nova
          Scotia.

No. 18.   Feit, D. M., 1987:   An Operational Forecast System for
          Superstructure Icing. Proceedings Fourth Conference
          Meteorology and Oceanography of the Coastal Zone. 4pp.

No. 19.   Esteva, D.C., 1988:   Evaluation of Priliminary Experiments
          Assimilating Seasat Significant Wave Height into a Spectral Wave
          Model. Journal of Geophysical Research. Vol. 93 No. C11,
          pp14,099-14,105

No. 20.   Chao, Y.Y., 1988:   Evaluation of Wave Forecast for the Gulf of
          Mexico. Proceedings Fourth Conference Meteorology and
          Oceanography of the Coastal Zone. pp.42-49

No. 21.   Breaker, L.C., 1989:   El Nino and Related Variability in Sea
          Surface Temperature Along Central California Coast. PACLIM
          Monograph of Climate Variability of the Eastern North Pacific and
          Western North America. (in press).

No. 22.   Breaker, L. C., and A. Bratkovich, 1989:   Oceanographic
          Conditions along the California Coast Surrounding the Period of
          the Puerto Rican Tanker Oil Spill. Journal of Geophysical
          Research. (Submitted).

No. 23.   Burroughs, L. D., 1989: Open Ocean Fog and Visibility Forecasting
          Guidance System. Technical Note/NMC Office Note No. 348.

No. 24.   Gerald, V. M., 1987:   Synoptic Surface Marine Data Monitoring.
          Technical Note/NMC Office Note No. 335, 10pp.

No. 25.   Breaker, L. C., 1989:   Estimating and Removing Sensor Induce
          Correlation form AVHRR Data. Journal of Geophysical Reseach.
          (in press)

No. 26.   Chen, H. S., 1988:   Infinite Elements for Water Wave Radiation
          and Scattering. International Journal for Numerical Methods in
          Fluids. (in press). 28pp.

No. 27.   Gemmill, W.H., T.W. Yu, and D.M. Feit, 1988: A Statistical
          Comparison of Methods for Determining Ocean Surface Winds. AMS
          Journal of Weather and Forecasting. Vol. 3, No. 2. pp153-160.

No. 28.   Rao. D. B., 1989: A Review of the Program of the Ocean Products
          Center. Weather and Forecasting. Vol. 4, pp. 427-443.

No. 29. Chen, H. S., 1989: Infinite Elements for Combined Diffration and Refraction . Conference Preprint, Seventh International Conference on Finite Element Methods Flow Problems, Huntsville, Alabama.

NO. 30. Chao, Y. Y., 1989: An Operational Spectral Wave Forecasting Model for the Gulf of Mexico. 2nd International Workshop on Wave Forecasting and Hindcasting. pp240-247.

No. 31. Esteva, D. C., 1989: Improving Global Wave Forecasting Incorporating Altimeter Data. 2nd International Workshop on Wave Forecasting and Hindcasting. 8pp.

No. 32. Richardson, W. S., J. M. Nault, D. M. Feit, 1989: Computer-Worded Marine Forecasts. Coastal Zone.

No. 33. Chao, Y. Y., T. L. Bertucci, 1989: A Columbia River Entrance Wave Forecasting Program Developed at the Ocean Products Center. Techical Note/NMC OFFICE NOTE 361.

No. 34. Burroughs, L. D., 1989: Forecasting Open Ocean Fog and Visibility. Proceedings 11th Conference on Probability and Statisitcs, Monterey, Ca., (in press).

No. 35. Rao, D. B., 1989: Local and Regional Scale Wave Models. Proceeding (CMM/WMO) Technical Conference on Waves. (in press)

No. 36. Chao, Y. Y., D. Duffy, 1989: Gulf of Mexico Wave Model. (in print).

No. 37. Burroughs, L. D., 1989: Ocean Products Center Products Review Summary. Technical Note/NMC Office Note No. 359. (in press) 29pp.

No. 38. Feit, D. M., 1989: Compendium of Marine Meteorological and Oceanographic Products of the Ocean Products Center (revision 1). NOAA Technical Memo NWS/NMC 68.

No. 39. Esteva, D. C., Y. Y. Chao, 1989: Directional Wave Spectra for the Labrador Extreme Wave Experimental (Lewex). APL Technical Report. (in press)